Regulation of Inverted Formin-1 (INF1) by Microtubule-Affinity Regulating Kinase 2 (MARK2)

Wojciech Kulacz

Thesis submitted to the Faculty of Graduate and Postdoctoral Studies in partial fulfillment of the requirements for the M.Sc. degree in Cellular and Molecular Medicine

Cellular and Molecular Medicine

Faculty of Medicine

University of Ottawa

Abstract

The actin and microtubule cytoskeleton plays a critical role in the establishment of cell polarity. Cell processes like mitosis and migration rely on the reorganization of the cytoskeleton to properly function. One driver of cell polarity is the formin, Inverted Formin-1 (INF1). INF1 is able to induce F-actin formation, activate the Serum Response Factor (SRF) pathway, stabilize microtubules, associate with microtubules, and disperse the Golgi body. Regulation of INF1 is unique, since it does not possess conserved formin regulatory domains. However, INF1 does possess many potential phosphorylation sites. In this study, we demonstrate that INF1's ability to induce F-actin stress fibers and activate SRF is inhibited by Microtubule-Affinity Regulating Kinase 2 (MARK2). Inhibition of INF1's actin polymerization activity by MARK2 likely occurs near INF1's C-terminus. However, MARK2 was unable to inhibit INF1's ability to stabilize microtubules, associate with microtubules, and disperse the Golgi. Furthermore, we show that INF1 overexpression is associated with primary cilium absence and in some cases, the presence of long cilia, suggesting that INF1 plays a role in primary cilium formation.

Table of Contents

List of Tables

CHAPTER 2: MATERIALS AND METHODS

List of Figures

CHAPTER 1: INTRODUCTION

CHAPTER 3: RESULTS PART I

CHAPTER 4: RESULTS PART II

List of Abbreviations

ADP……Adenosine Diphosphate
αTAT1……Alpha-tubulin acetyltransferase
AMPK……..AMP-activated protein kinase
aPKC……atypical Protein kinase C
ATP……....Adenosine Triphosphate
ARP 2/3……Actin Related Proteins 2 and 3
DAAM……Disheveled-associated activators of morphogenesis
DAD……..Diaphanous Autoinhibitory Domain
DAPI……..4',6-diamidino-2-phenylindole
DBS……Donor Bovine Serum
Dia……..Diaphanous
DMEM……Dulbecco's Modified Eagle Medium
DID……Diaphanous Inhibitory Domain
F-Actin……..Filamentous actin
FBS……Fetal Bovine Serum
FP……....Fluorescent Protein
FH……..Formin Homology
FHOD……Formin Homology Domain-Containing Protein
FMN……Formin
FRL……Formin Related Gene in Leukocytes
G-Actin……..Globular actin
GAP……GTPase-activation protein
GBD……..GTPase Binding Domain
GDP……..Guanosine Diphosphate
GEF……..Guanine nucleotide exchange factor
GSK-3β……Glycogen Synthase Kinase 3β
GTP……..Guanosine Triphosphate
HDAC……Histone deacetylase
IFT……Intraflagellar Transport
INF……Inverted Formin
MAPK……Mitogen-activated protein kinase
MAPs……Microtubule associated proteins
MARK……Microtubule affinity-regulating kinase
MAL……...Myocardin-associated protein
MDCK……..Madine-Darby Canine Kidney Cell
MEK1……...Mitogen-Activated Protein Kinase (MAPK) kinase
MRTF……Myocardin-Related Transcription Factor
MT……..Microtubules
MTBD……...Microtubule Binding Domain
MTOC……Microtubule Organizing Center
PBS……Phosphate Buffer Saline
PLK……Polo-like kinase
PTM……Post-translational modifications

ROCK……..…..…Rho-associated kinase
siRNA…….…...…Small Interfering Ribonucleic Acid
SRE……..…..……Serum Response Element
SRF…….……..…Serum Response Factor
+TIPS…….……..…Plus-end tracking proteins
WASP…….……Wiskott-Aldrich syndrome protein
WH2……...……WASP Homology two
YFP…….……...…Yellow fluorescent protein

Acknowledgments

I am grateful for the support and motivation of my supervisor, Dr. John Copeland. I appreciate his advice, patience, and enthusiasm throughout my graduate studies. His scientific knowledge and devotion to research were constant reminders and an inspiration to persevere at difficult times. In addition, I would like to thank my thesis advisory committee, Dr. Robert Screaton and Dr. Johnny Ngsee, for their guidance throughout my project.

I recognize and value the numerous members of the Copeland lab. I am grateful for the work done by Kevin Young, who conducted the preliminary experiments which led to the motivation for this thesis. I would like to thank Susan Thurston and Sarah Copeland for training me and being a part of the INF1 team. Their expertise and large contributions to the lab were invaluable to my progress. In addition, I would like to thank Christine P, Allan, Faduma, and Christine T as well the many other students who have passed through the Copeland lab for their friendship and hard work.

I am thankful for the support I have received from the Department of Cellular and Molecular Medicine, especially from the lab of Dr. S Lee. I would like to specifically thank Tim Audas for his expertise, as well as many of the friends I have made there, especially Mathieu and Camille.

Finally, I would like to thank my parents for their constant motivation and for reminding me of the value of hard work and dedication.

Chapter 1: Introduction

The establishment of cellular polarity is necessary for numerous physiological functions from mitosis to cell migration. These processes are dependent on the reorganization of cellular components, including the cytoskeleton. Cytoskeletal rearrangements, driven by internal and external cues, give rise to a polar distribution of organelles and intracellular proteins, which are fundamental in many cell processes.

Three types of filaments compose the cytoskeleton: microtubules, actin filaments, and intermediate filaments, all of which have unique subunits and functions. Microtubules and actin filaments drive cell polarity, and thus the importance of proteins that regulate these two structural systems play critical roles. Formins have emerged as key players in the polarity field due to their roles as regulators of the actin cytoskeleton. In particular, Inverted Formin-1 (INF1) has been identified as a potential driver of polarity due to its ability to directly regulate actin and microtubule dynamics. Yet, unlike the other formins, the mechanisms that control INF1 activity are unknown. This thesis investigates the potential regulation of INF1 by the kinase MARK2.

1.1. The Actin Cytoskeleton

Maintaining and regulating the cytoskeleton plays an important role in many cell processes including motility, adhesion, and division. The dynamic organization of the actin cytoskeleton regulates cell morphology, protein trafficking, and organelle distribution.

Actin is the most abundant intracellular protein and exists in two forms: globular (G-actin) and filamentous (F-actin). The assembly of actin filaments is important in the

formation of many cellular structures. F-actin is a main component of microvilli, lamellipodia, filopodia, the cell division contractile ring, and stress fibers.

The rate-limiting step of actin polymerization is nucleation. The formation of an initial actin dimer or trimer complex is kinetically unfavourable due to the instability of actin multimers and sequestration of actin monomers by numerous proteins (reviewed in Nur Firat-Karalar and Welch, 2011). Profilin sequesters G-actin, inhibiting it from nucleation, while Thymosin β_4 sequesters actin and inhibits its incorporation into F-actin. However, above a certain critical concentration of monomers, G-actin dimers and trimers will begin to spontaneously polymerize. Though the process of nucleation is kinetically unfavourable and the resulting complex unstable, cells are able to rely on actin nucleating proteins such as formins, spire, or Arp2/3for filament nucleation. Following nucleation, ATP-bound G-actin is preferentially added to the 'barbed end' or plus end of the growing filament, while subunits preferentially dissociate from the 'pointed end' or minus end, a process known as "treadmilling". This occurs because the critical concentration for monomer addition is much higher at the pointed end than the barbed end. After monomer incorporation, bound ATP is hydrolyzed into ADP, destabilizing the filament as a consequence (Pollard and Cooper, 2009). The resulting one-directional incorporation of G-actin forms a polarized actin filament.

Numerous proteins regulate the assembly of f-actin. Profilin catalyzes the exchange of bound ADP for ATP by G-actin and also binds to actin nucleators, to act as a shuttle by bringing actin monomers to the extending filament. Conversely, cofilin binds G-actin-ADP at the pointed end of filaments, causing depolymerization and preventing reassembly. Cofilin also severs F-actin, generating more barbed ends on filament

fragments, and also allowing for monomeric actin recycling. Lastly, the capping protein CapZ promotes disassembly at the plus end, while Tropomodulin stabilizes the filament at the minus end. (Lodish et al., 2004).

Perhaps the most important regulatory components of F-actin assembly are actin nucleating proteins. In their absence, formation of the actin filament relies on spontaneous nucleation, a kinetically unfavourable event. The Arp2/3 complex is an actin nucleator that mimics the barbed-end of an actin filament. Arp2/3 attaches itself to an existing filament, forming a new branched filament at a 70º angle, a process referred to as autocatalytic branching (Goley and Welch, 2006). Spire proteins are actin nucleators that contain four Wiskott-Aldrich syndrome protein (WASP)-homology-2 (WH2) domains which act as platforms to bind individual G-actin monomers (Quinlan et al., 2005). The tetramer scaffold becomes an initiation site for the assembly of unbranched actin filaments and spire remains attached to the pointed end of the filament, capping it to prevent depolymerization. Similar to spire proteins, formins are actin nucleators that promote the assembly of unbranched actin filaments. A dimer of Formin Homology 2 (FH2) domains binds to and stabilizes the actin dimer. Following nucleation, formins remain attached to the growing barbed end, capping them yet allowing the filament to extend through sequential bind-and-release interactions (Zigmond, 2003).

1.2. Actin Stress Fibers

Fluctuation of cell body size and cell movement in non-muscle cells is directed through numerous contraction and expansion events, one being the formation of actin stress fibers. These fibers are composed of 10-30 actin filaments held together in a thick bundle by the crosslinking protein α-actinin (Lazarides and Burridge, 1975). Contractile

forces are generated by bundles of Myosin-II motor proteins, which traverse along the actin and allow stress fibers to slide past each other (Pellegrin and Mellor, 2007).

Three subpopulations of actin stress fibers exist in fibroblasts, classified by their location: Ventral stress fibers, which are anchored at both ends to integrin-rich focal adhesions along the base of the cell by the proteins zyxin, vinculin, talin, and paxillin; Dorsal stress fibers are anchored to the base of the cell at one end only by a focal adhesion, with the other end extending into the cytosol as loose actin filaments; Transverse arc stress fibers are structurally aligned to protruding lamellipodia, forming an arc shape just below the dorsal surface of a migrating cell, and later collapsing back towards the nucleus to be recycled (Burridge, 1986, Small, 1998). Each stress fiber population also assembles in a distinct way. Ventral stress fibers assemble by joining two stress fibers, each individually anchored to a focal adhesion. Dorsal stress fibers extend from focal adhesions, while transverse stress fibers form by the adhesion of short actin bundles to myosin bundles (Hotulainen and Lappalainen, 2006). The various stress fiber structures, and their anchoring to focal adhesions, provide mechanical force and structural integrity for the cell.

Formation of stress fibers is under the control of the Rho family of GTPase signaling proteins, primarily RhoA. RhoA activates Rho kinase I and II (ROCKI and II), as well as the formin, mammalian Diaphanous-1 (mDia1) (Watanabe et al., 1999). ROCK I promotes the activity of non-muscle Myosin II through phosphorylation, while both ROCK I and II may participate in the activation of the LIM-kinase pathway by inhibiting cofilin (Maekawa et al., 1998; Pritchard et al., 2004). mDia1 promotes the activity of the actin-monomer binding and F-actin assembly protein profilin (Kovar et al., 2005).

Depletion of mDia1 is marked by a reduction in actin stress fibers, which may be partially rescued by redundancy that exists among the other formins (Hotulainen and Lappaleinen, 2006; Chhabra and Higgs, 2007).

1.3. Serum Response Factor (SRF)

Beyond effects on the actin and microtubule cytoskeletal networks, formins also induce activation of the actin/MAL/SRF transcriptional response (Figure 1.1). In fibroblasts, the assembly of actin filaments mediated by Rho GTPases depletes the cytosolic pool of G- actin. This results in the translocation of the SRF cofactor MAL (myocardin-related transcription factor A), into the nucleus. MAL then binds the SRF protein at the SRF promoter, inducing the transcription of a variety of target genes some of which encode cytoskeletal components, e.g. β-actin and vinculin (Sotiropoulos et al., 1999; Copeland and Treisman, 2002; Miralles et al., 2003; Copeland et al., 2004).

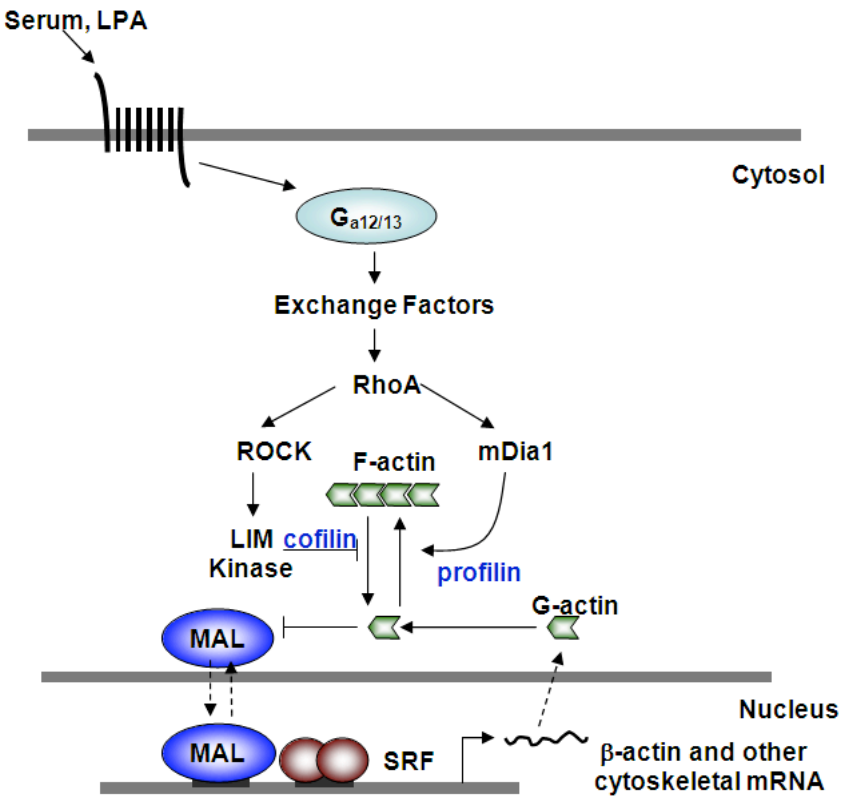

Figure 1.1. The actin/MAL/SRF pathway in fibroblasts

F-actin accumulation may be stimulated through Rho-GTP via two pathways. RhoA activates its downstream effector, Rho-associated Kinase (ROCK) through phosphorylation, leading to the inactivation of the F-actin severing protein, cofilin. RhoA also activates Diaphanous (mDia1), by alleviating autoinhibition, therefore stimulating F-actin assembly. The subsequent G-actin depletion allows MAL to shuttle to the nucleus, where it acts as an SRF cofactor, triggering the transcription of cytoskeletal mRNA.

1.4. Microtubule Network

Microtubules play an essential role in intracellular trafficking, cell division, cell migration, extracellular sensing, and organelle positioning. Microtubules are made of α/β heterodimers arranged in a polarized head-to-tail orientation forming a protofilament. Standard microtubules are composed of 13 protofilaments arranged in a ring, called a 'singlet'. Specialized structures such as flagella and cilia are made from an arrangement of 'doublet' microtubules – a singlet ring with an adjacent set of ten protofilaments. Both flagella and cilia are composed of an axoneme of nine outer doublet microtubules which surround a pair of central singlets. Meanwhile, centrioles and basal bodies are made of 'triplet' microtubules, a set of 10 additional protofilaments linked to a doublet (Lodish et al., 2004).

Organization of microtubules is under the control of the microtubule-organizing centre (MTOC). In animals, the centrosome acts as the main MTOC, but other structures such as cortical membranes, the Golgi complex, and the nuclear envelope of myotubes have been identified as secondary MTOCs (Luders and Stearns, 2007). The MTOC is the site of nucleation (γ-tubulin is localized here) and often remains the anchor for growing microtubules (Wade and Hyman, 1997). A γ-tubulin ring complex (γ-TuRC) acts as a scaffold and cap for the nucleation of new tubulin filaments at the minus (-) end (Kollman et al., 2011). GTP-bound tubulin heterodimers are added first longitudinally along the growing protofilament, and then laterally to enhance stabilization. Following dimer addition, the GTP bound to the β-subunit acts as a capping protein until it is hydrolyzed into GDP, resulting in microtubule depolymerization. A high concentration of free GTP β-tubulin promotes polymerization by maintaining the GTP-cap before it can be

hydrolyzed into GDP. Low concentrations of GTP β-tubulin lead to microtubule depolymerization. This differing rate of dimer incorporation and GTP hydrolysis at the plus end of microtubules is termed 'dynamic instability' (Hammond et al., 2009).

1.5. Microtubule Associated Proteins (MAPs)

The regulation of microtubule integrity is under the control of several stabilizing and destabilizing proteins, called microtubule-associated proteins (MAPs). Proteins such as MAP1 and MAP4 assemble and stabilize microtubules, while MAP2 crosslinks microtubules to intermediate filaments. Other MAPs link the cytoskeleton to various structures. For example, Clip-170 cross-links microtubules to endosomes and chromosomes. Many stabilizing MAPs also possess multiple tubulin dimer binding site repeats, enabling them to cross-link microtubules. Meanwhile, proteins like katanin, destabilize and cut microtubules into severed fragments (Roll-Mecak and McNally, 2010).

Two important MAPs are found in neurons: MAP2, which is localized to dendrites, and Tau, localized to axons. Both proteins contain a positively-charged microtubule binding domain that binds to the negatively-charged C-terminus of tubulin, and an acidic projection domain that extends outward from the microtubule. MAP2 and Tau use their N-terminal projection domain to assist the movement of microtubule transport proteins by mechanical separation of microtubules. However, at high concentrations, MAP2 and Tau prevent adequate transport along microtubules by blocking motor protein binding sites and trafficking routes (Ackmann et al., 2000).

In vivo, Tau associates with a pool of highly dynamic microtubules that are susceptible to depolymerization through the action of drugs. Tau is subjected to a number

of post-translational modifications (PTM). For example, Tau may be phosphorylated by a number of protein kinases, including GSK3β, CDK5, MARK1-4, and MAPK (Augustinack et al., 2002; Mi and Johnson, 2006). Phosphorylation of Tau on its microtubule-binding domain (MTBD) results in its dissociation from negatively charged tubulin (Cash et al., 2003). Hyperphosphorylation of Tau leads to its accumulation and the formation of neurofibrillary tangles (NFTs), a marker of Alzheimer's disease (Grundke-Iqbal et al., 1986).

Cell polarity is also dependent on microtubule-associated proteins. Plus-end tracking proteins (+TIPs) like CLIP170 associate with the growing tip of microtubules. CLIP170 links microtubules to endocytic vesicles, allowing them to be trafficked throughout the cell (Valetti et al, 1999). In addition, +TIPS may pull on stable microtubules and therefore the MTOC, which is anchored to microtubule minus ends, leading to cell reorientation (Galjart, 2005).

1.6. Microtubule Modifications

The formation of complex microtubule structures such as cilia or basal bodies relies on numerous tubulin post-translational modifications (PTM). These modifications create an assorted subset of tubulin monomers that promote the assembly of specific protein complexes, enabling microtubules to engage in particular functions.

Some specialized sets of microtubules undergo the polymodifications of glutamylation and glycylation, which involves the fusion of glutamate or glycine amino acids to an exposed glutamate residue on the C-terminal tails of both α- and β-tubulin (Verhey and Gaertig, 2007). Cilia and flagella contain a population of glycylated microtubules, while neuronal cells, centrioles, and the mitotic spindle are heavily

glutamylated (Redeker et al., 2005). In *Tetrahymena*, the absence of the C-terminal region of β-tubulin, which is normally heavily glycylated, leads to non-motile and short cilia, while in *Drosophila* it impedes the formation of sperm axonemes (Redeker, 2004; Dossou et al., 2007).

Microtubule acetylation is a PTM involving the addition of an acetyl group to tubulin, and is associated with populations of stable microtubules. Acetylation occurs on the lysine-40 residue of α-tubulin subunits, which is located on the luminal surface of microtubules. Modification by alpha-tubulin acetyltransferase-1 (αTAT1) promotes greater affinity of motor proteins, such as kinesin-1 to microtubules (Akella et al, 2010; Reed et al., 2006). Histone Deacetylase 6 (HDAC6) and Sirtuin 2 (Sirt2) have been shown to deacetylate microtubules and are involved in microtubule-dependent cell motility and in the mitotic exit of the cell cycle, respectively (Dryden et al., 2003; Hubbert et al., 2002).

Besides acetylation, stable microtubules are also modified by detyrosination, where the C-terminal tyrosine of α-tubulin is severed by a carboxypeptidase. The function of detyrosination is unclear, however, an increase in detyrosinated microtubules is associated with increased tumorigenesis and tumour invasiveness (Lafanechere et al., 1998). Similar to acetylated microtubules, kinesin-1 also has a preference in binding to detyrosinated microtubules compared to tyrosinated microtubules (Dunn and Peckham, 2008).

1.7. A Link Between Actin Filaments and Microtubules

The first observation of the actin and microtubule cytoskeleton being structurally linked came *in vitro* when actin bundles were shown to move via motor proteins along

microtubules in the presence of cytosolic factors (Waterman-Storer and Bement, 2000). Some proteins that possess actin and microtubule binding domains are: the budding yeast protein Bim1, which transports astral microtubules along actin tracks during cytokinesis (Hwang et al., 2003); the Myo5a-kinesin complex, which mediates organelle trafficking along both microtubules and actin (Huang et al., 1999); and MAP2c, which promotes microtubule growth and actin bundling (Ozer and Halpain, 2000). These crosslinkers are important in numerous cell processes. Microtubule-actin interactions have been associated with lamellipodium ruffling in migrating cells, where microtubules are transported towards the cell center in an actomyosin dependent process (Waterman-Storer and Salmon, 1997). Similar interactions occur during wound healing, where microtubules are dragged to the wound border through association with flowing actin filaments (Mandato and Bement, 2003). Formins also have a broad role in microtubule dynamics, with mDia1 being involved in microtubule stabilization, actin alignment, centrosome orientation, and spindle positioning (Bartolini and Gundersen, 2009). Specific domains of mDia1 such as the FH1 and FH2 domains, along with protein cofactors allow for this activity.

Interactions between the actin and microtubule cytoskeleton are also mediated by MAPs during the establishment of cell polarity. CLIP170 interacts in-vitro with IQGAP1, which colocalizes with actin at the leading edge of polarized cells (Fukata et al., 2002). Overexpression of IQGAP1 induces the formation of multiple leading edges, characterized by the buildup of microtubules and actin filaments at filopodia. Another actin-microtubule crosslinking protein, ACF7, is responsible for anchoring microtubules at actin-rich cortical areas (Kodama et al., 2003).

1.8. Formin Homology Proteins

Formins are a set of cytoskeletal remodeling proteins that are required to establish and maintain proper microtubule organization, cell polarity, stress fiber formation, cell division, and vesicular trafficking (Higgs, 2005). There are 15 mammalian formins that can be divided into seven sub-families: Diaphanous (Dia), Dishevelled-associated activator of morphogenesis (DAAM), Formin-related proteins in leukocytes (FRL), Formin homology domain-containing protein (FHOD), Inverted formin (INF), Formin (FMN), and Delphilin. Within each group there may be multiple genes and splice variants (Higgs, 2006).

Formins are identified by the presence of two structurally and functionally conserved domains, Formin-homology 1 (FH1) and Formin-homology 2 (FH2). The FH1 domain binds profilin, a G-actin binding protein. Profilin prevents spontaneous actin nucleation while FH1-bound profilin-actin increases the rate of formin-regulated actin polymerization (Zigmond, 2004). The FH2 domain homodimerizes and nucleates *de novo* actin polymerization by binding G-actin. The exact model for FH2 binding to F-actin barbed ends is still contested. The current theory proposes that one FH2 monomer is bound to an actin subunit on the growing barbed end, while the other FH2 monomer is free to accept an incoming G-actin monomer, thereby acting as a "leaky capper" (Moseley et al., 2004, Park and Pollard, 2009). During F-actin elongation, the FH2 domain shifts between an open and closed conformation. While in an open conformation, it incorporates G-actin at the growing barbed-end of the filament. In a closed conformation, the FH2 domain blocks binding of capping proteins and depolymerization at the barbed end of F-actin (Zigmond, 2004, Park and Pollard, 2009). Rates of actin

nucleation differ amongst formins. mDia1 and mDia2 are strong actin nucleators, whereas FRL1 is considered to be a weak nucleator (Higgs, 2005). Many formins are regulated through conserved auto-inhibitory mechanisms, with regulation of Diaphanous Related Formins (DRFs), being best understood. In an auto-inhibited conformation, the N-terminal Diaphanous Inhibitory Domain (DID) of DRFs interacts with the C-terminal Diaphanous Autoregulatory Domain (DAD) (Figure 1.2). Formin auto-inhibition is alleviated by the binding of a GTP-bound Rho molecule to a GTPase binding domain (GBD) that partially overlaps with the DID, preventing interaction between the DID and DAD (Li and Higgs, 2005). Formins may be activated by many GTPases. For example, mDia1 may be activated by RhoA, B, or C, mDia2 is activated by Rho A and Cdc42, and FHOD1 is activated by Rac1 (Watanabe et al., 1999; Alberts, 2000, Peng et al.; 2003, Gasteier et al., 2003). Although many non-DRFs are autoinhibited, their regulatory mechanisms remain unknown because they do not possess conserved formin regulatory domains (Higgs and Peterson, 2005).

1.9. Inverted Formin-1 (INF1)

Our laboratory identified INF1 as a novel microtubule-associated formin. The conserved FH1 and FH2 domains of INF1 are located in the N-terminus, unlike other formins where these are found in the C-terminal end (Figure 1.3). As in other formins, the FH2 domain of INF1 is both necessary and sufficient to induce F-actin stress fiber formation in serum-starved cells. (Young *et al*., 2008). INF1 contains a C-terminal microtubule binding domain (MTBD) and preliminary data from our lab suggests that INF1 also binds and bundles F-actin. However, INF1 does not possess any of the

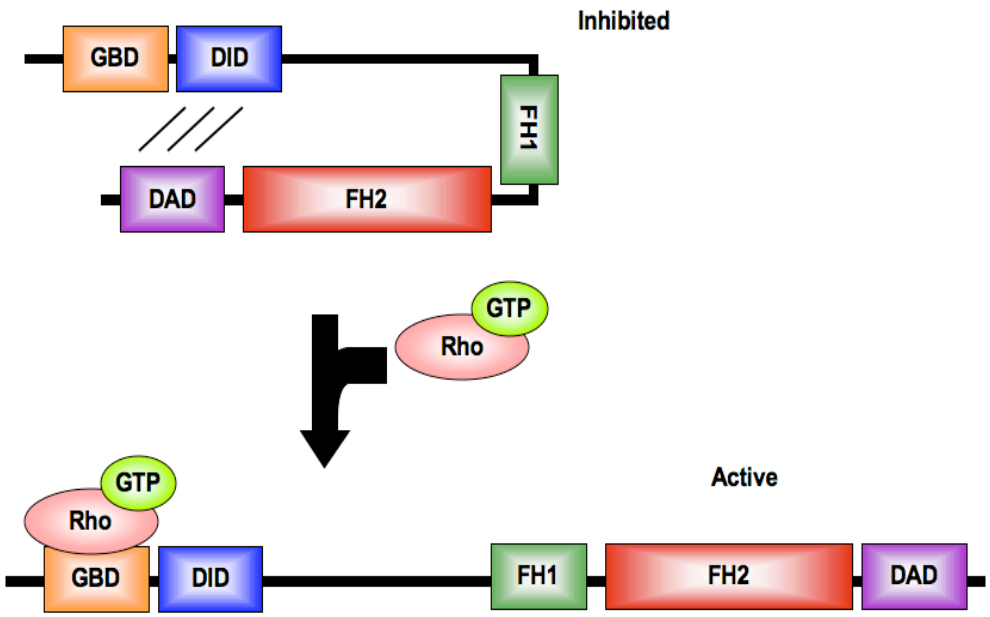

Figure 1.2. Diaphanous-Related Formins are regulated through auto-inhibition

The Diaphanous Inhibitory Domain (DID) interacts with the Diaphanous Autoregulatory Domain (DAD) to autoinhibit DRFs. Autoinhibition is alleviated through the binding of GTP-bound Rho to the GTPase Binding Domain (GBD).

previously described formin regulatory domains (Young et al., 2008). INF1 over-expression induces microtubule stabilization and acetylation; knockdown of INF1 expression results in the depletion of acetylated tubulin (Young et al., 2008). Surprisingly, structure/function analysis of INF1 demonstrates that the MTBD is sufficient, but not essential for INF1-induced MT acetylation (Young et al., 2008). Instead, in the absence of the MTBD, the FH1 and FH2 domains are both necessary and sufficient for this process. This activity is not unique to INF1, as the FH1 and FH2 domains of a handful of other formins are sufficient to induce MT acetylation and detyrosination (Thurston, unpublished data; Bartolini et al., 2008,). As discussed above, MT acetylation has been shown to have a regulatory effect on many cell functions such as protein-trafficking and is required for the induction and maintenance of neuronal polarity (Hammond et al., 2008).

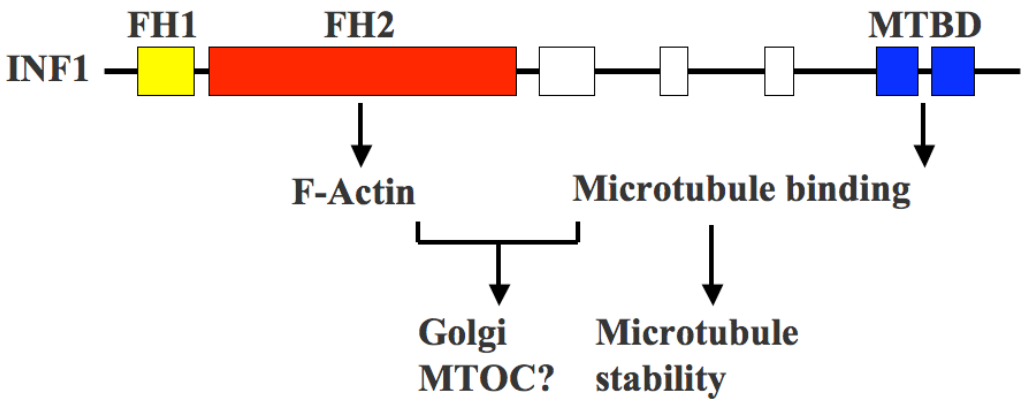

Figure 1.3. Schematic of INF1's functional domains

INF1 is characterized by its N-terminal FH1 and FH2 domains, and its C-terminal MTBD. The FH2 mediates F-actin polymerization and SRF activity, and is also necessary for Golgi dispersion, while the MTBD associates with microtubules. Microtubule stability is induced by the FH1/FH2 domains and the MTBD.

1.10. The Establishment of Cell Polarity

Induction of cell polarity through formation of an asymmetric microtubule network is essential for numerous processes such as cell migration and cell division. The initial steps of cell migration include the extension of the cell membrane through the actin-dependent formation of lamellipodia and filopodia. These structural protrusions attach to the extracellular matrix through integrins which provide the tracks for cells to move along.

The leading edge of the cell is a zone of mass actin polymerization. The Arp2/3 complex is the main player in lamellipodia formation due to its ability to form branched networks of actin filaments, and is likely under the control of Rac. Meanwhile spire and formins are active in filopodia extension, a process controlled by Cdc42 (Astin et al., 2010, Ridley, 2011). Inhibition of either Rac or Cdc42 has been shown to prevent the establishment of cell polarity (Kroschewski et al., 1999).

Changes in organelle orientation are also hallmarks of cell polarity. During directional cell migration, the Golgi and MTOC reposition themselves between the nucleus and the leading edge of fibroblasts. However, rearward movement of the entire nucleus by actin and myosin II has also been documented. In this case, the MTOC remains immobile (Gomes et al., 2005). Conversely, in T-cells, the MTOC is reoriented to face the target cell, a process dependent on the formins Dia1 and FRL1 (Kupfer et al., 1983, Gomez et al., 2007).

Myotonic dystrophy kinase-related Cdc42 binding kinase (MRCK) and the Par6/Par3/aPKC polarity complex have also been shown to influence nuclear and MTOC movement through myosin II and dynein/dynactin activation, respectively (Ridley et al.,

2003; Gomes et al., 2005). Using nocodazole to inhibit dynamic microtubules Mikhailov and Gundersen, (1998) showed that MTOC reorientation was microtubule dependent.

Golgi reorientation is actin and MT dependent and Golgi subcellular localization can be used as a reporter of cell polarity. Reorientation of the Golgi is a feature of cell polarization, while Golgi fragmentation is also a standard process during mitosis. In late prophase, the Golgi disperses into mini-stacks, a necessary step for the Golgi's eventual equal distribution to daughter cells (reviewed in Nelson, 2000). Mediating this fragmentation are MEK1 and PLK, which phosphorylate the Golgi stacking proteins Grasp55 and Grasp65, respectively (Acahrya et al, 1998; Sutterlin et al., 2001). Once the Golgi is dispersed, Golgi proteins like Grasp65 and GM130 become free to regulate mitosis, where both are involved in the regulation of spindle formation (Sutterlin et al., 2005; Kodani and Suterlin, 2008).

The Golgi has been shown to arrange itself in front of the nucleus and towards the leading edge in migrating NIH-3T3 fibroblasts. This rearrangement has been shown to be both actin and microtubule dependent (Magdalena et al, 2003; Thyberg and Moskalewski, 1999). Meanwhile, maintenance of the Golgi ribbon structure is also microtubule dependent, as microtubule depolymerization leads to Golgi fragmentation (Thyberg and Moskalewski, 1999).

Recent observations indicate that the Golgi itself may serve to establish cell polarity. A subset of microtubules radiate from the Golgi, pointing asymmetrically towards the leading edge of the cell (Efimov et al, 2007; Chabin-Brion et al., 2001). Microtubule nucleation at the Golgi is dependent on AKAP450, which binds to the cis-Golgi protein GM130, providing a platform for direct interaction with the γ-TuRC

complex (Rivero et al., 2009). Meanwhile, the microtubule network is also essential to maintain the structure of the Golgi ribbon. Treatment with the microtubule depolymerization drug colcemid fragments the Golgi, indicating that microtubules are required to maintain the Golgi ribbon (Wehland et al., 1983).

1.11. INF1 and Cell Polarity

Preliminary results in our lab show that endogenous INF1 colocalizes with the Golgi in polarized cells. Over-expression of full-length INF1 induces dispersion of the polarized Golgi ribbon into mini-stacks that are distributed throughout the cytoplasm. This dispersion is dependent upon the function of both the FH2 and MTBD of INF1, suggesting that it is the coordinated regulation of actin and MT dynamics that is required for this effect (Sarah Copeland, personal communication). We propose a model where INF1 may play a role in cell polarity through its ability to regulate directly actin and microtubule organization and thereby affect Golgi subcellular distribution.

1.12. Regulation of INF1 and Microtubule-affinity regulating kinases (MARKs)

INF1 does not possess any of the previously described formin regulatory domains (Young et al., 2009). However, it does contain two consensus K-X-G-S motifs recognized in other MAPs by the serine/threonine kinase MARK2. MARK2 belongs to the adenosine monophosphate-activated protein kinase-related kinase (AMPK-RK) family of proteins. Four mammalian MARK proteins (MARK1-4) have been identified. They share roughly 45% homology and possess a number of conserved structural domains (Matenia *et al*, 2009). MARKs phosphorylate microtubule-associated proteins

(MAPs) at K-X-G-S sites (corresponding to the general K/R-X-X-S/T AMPK consensus) to inhibit MAP-microtubule interactions.

The MARK orthologs, the Par-1 proteins, are involved in a variety of cellular and developmental contexts and are part of the Par polarity regulating pathway. Together, the six Par genes were shown in genetic screens to be necessary for proper partitioning of the cytoplasm in *C.elegans* embryos during anterior-posterior establishment and in establishing epithelial cell polarity in mammals. Par-1 and Par-4 are serine-threonine kinases, while other Par proteins have signal scaffolding domains (Levitan et al, 1994, Watts et al, 2000). Par-1 is an effector of the aPKC/Par3/Par6 polarity complex, which localizes to tight junctions of epithelial cells. aPKC phosphorylates Par-1b, the MARK2 ortholog, allowing it to diffuse throughout the cytoplasm and potentially interact with other effectors (Hurov et al., 2004). The absence of Par-1b results in the removal of cells from the epithelial monolayer in MDCK cells (Suzuki et al, 2004). This may be due to a lack of microtubule stabilization at the lateral membrane. In hippocampal neurons, knockdown of Par-1b resulted in Tau dephosphorylation and the formation of multiple axons, indicating that Par-1b plays an essential role in axon-dendrite polarity establishment (Chen et al., 2005).

An in vitro kinase assay conducted in collaboration with the Screaton lab suggested that the INF1C-terminus is a MARK2 substrate. In preliminary experiments, INF1-induced microtubule acetylation was inhibited by coexpression of MARK2 (Kevin Young, unpublished results). In section 3.1, I investigate the ability of MARK2 to regulate the effects of INF1 on cytoskeletal dynamics and Golgi morphology.

1.13. The Primary Cilium

The primary cilium acts as a sensory apparatus for the cell, transmitting extracellular signals back to the cell body. In renal epithelium, primary cilia are bent in the direction of extracellular fluid flow, activating calcium signaling (Rydholm et al., 2010). Disruption of ciliary function leads to cyst formation in the kidney and polycystic kidney disease (Berbari and Yoder, 2009). Cilia also have functions in light and odour detection, as well as in limb development (Abd-El-Barr et al., 2007,Kulaga et al., 2004, Haycraft et al., 2005).

The formation of cilia only occurs in quiescent cells and cilia are disassembled upon re-entry into the cell cycle. The foundation of cilia is formed by the triplet microtubule structure of "mother centriole" basal bodies. Primary cilia lack the central pair of doublet microtubules present in motile cilia. Cilia extension occurs by the addition of tubulin to the plus-end of two of the three triplet microtubules, creating a doublet microtubule axoneme. Extension at microtubule plus-ends, and a lack of protein synthesis within the cilia, makes Intraflagellar Transport (IFT) essential. IFT proteins are moved from the cell body to the tip of the cilia via kinesin-2 motors while dynein-2 motor proteins drive transport from the cilia back to the cell (Rosenbaum and Whitman, 2002; Scholey, 2003). Numerous IFT complexes have been identified, and mutations in these complexes result in shortened cilia, stunted bulging cilia, or the absence of cilia altogether (Brazelton et al, 2001; Hou et al., 2007; Pazour et al., 2000; Iomini et al, 2009).

Cilia are rich in both acetylated and detyrosinated microtubules. The tubulin acetylase αTAT1 is required for microtubule acetylation and primary cilium formation in

mammals (Shida et al, 2010). In contrast, the tubulin deacetylase HDAC6, induces disassembly of the primary cilium (Pugacheva et al, 2007). INF1 overexpression induces increased microtubule acetylation and therefore we looked at how INF1 expression may affect cilia structure.

Chapter 2: Materials and Methods

2.1 Cell Culture

NIH-3T3 mouse fibroblasts were cultured in Dulbecco's Modified Eagle Media (DMEM, ATCC), supplemented with L-Glutamine, and 10% Donor Bovine Serum (DBS). "Kyoto" HeLa cells were obtained from the laboratory of Dr. Laura-Trinkle Mulcahy and cultured in DMEM (Invitrogen) supplemented with Glucose, L-Glutamine, Sodium Pyruvate, and 10% Fetal Bovine Serum (FBS). Both cell lines were grown in a 5% CO_2, 37ºC incubator and used until passage 15.

2.2 Immunofluorescence

NIH-3T3 cells were seeded at a density of 125,000 cells/well of a 6-well plate on acid-treated coverslips, on the day before transfection. Cells were roughly 80% confluent on the day of transfection. A total of 1.5μg of DNA was mixed with Optimem media (Gibco), and 5μL of polyethylenimine transfection reagent (PEI) (Polyscience). The DNA-PEI complex was incubated for 30mins at room temperature and added to optimem-washed cells in a dropwise fashion. Following 5hrs of incubation, cell culture media was changed to either DMEM + 0.5%DBS (for actin stress fiber and acetylated tubulin assays) or DMEM+ 10%DBS (microtubule affinity and golgi dispersion assays). For "Kyoto" HeLa cells, cell culture media contained FBS and not DBS. Cells were fixed in either 100% methanol for 10 minutes or 4% Paraformaldehyde in PBS for 15 minutes. Cells were permeabilized for 10 minutes with 0.3% Triton X-100, plus 10% FBS in PBS. Cells were then incubated with primary antibodies (Table 2.1) in 5% FBS in PBS at room temperature. After 1 hour, cells were washed 3X in PBS and incubated with secondary antibodies (Table 2.1) in 5% FBS in PBS at room temperature for 1 hour. Cells were

washed as before in PBS and then mounted with Vectashield mounting media (Vector Labs) with or without DAPI. Stained cells were visualized on a Zeiss Axio Imager Z1 microscope using an AxioCam HRm camera. Images were obtained by using a 63X Plan Apochromat objective and processed using Axiovision software. Optical sections were obtained by using an apotome.

Table 2.1: Antibodies

Mouse anti-Flag 10μg/mL (Sigma)	Mouse anti-GM130 1.3μg/mL (BD Biosciences)
Rabbit anti-Flag 2μg/mL (Sigma)	Donkey anti-Rabbit Cy3 7.5μg/mL (Jackson Immunoresearch)
Mouse anti-Myc 5μg/mL (Santa Cruz)	Donkey anti-Mouse Cy5 15μg/mL (Jackson Immunoresearch)
Rabbit anti-Myc 0.4μg/mL (Santa Cruz)	Goat anti-Rabbit Cy5 15μg/mL (Jackson Immunoresearch)
Mouse anti-tubulin 0.4μg/mL (Santa Cruz)	Donkey anti-Mouse 488 7.5μg/mL (Jackson Immunoresearch)
Mouse anti-acetylated tubulin 1.6μg/mL (Sigma)	Fluorescein-Phalloidin 0.5μM (Molecular Probes)

2.3 Serum Response Factor (SRF) Assay

NIH 3T3 cells were seeded as previously described. Cells were transfected with 50ng of the 3DA.Luciferase reporter construct, 250ng of the MLV-LacZ reference plasmid, and indicated expression constructs. As previously noted, empty vector was used to equate each transfection to 1.5μg of DNA per well in a 6-well dish. 0.1μg of an

SRF positive control plasmid (SRFVP16) was included as a positive control. Transfections were completed using Optimem and PEI as previously described. After 5hrs of incubation with DNA, media was changed to 0.5%DBS in DMEM. After 24 hours, cells were harvested using standard protocol for B-Gal and luciferase assays. Cells were washed in 1X PBS and scraped into 500μL of 1X PBS. Cells were then centrifuged at 5000rpm at 4ºC for 5mins. The pellet was resuspended in reporter lysis buffer (Promega), and frozen overnight at -20ºC. Samples were thawed at 37ºC and vortexed to ensure complete cell lysis. The lysates were then centrifuged at 13,000 rpm for 10 minutes to remove cell debris. The supernatant was transferred to a new tube. Luciferase assays were completed by adding 40μL of luciferin to 40μL of protein lysate. β-Gal reactions were completed by adding 200μl of 4mg/mL chlorophenol red β-D galactopyranosidase (CPRG- Calbiochem) diluted 1:10 in β-Gal buffer (10mM $MgSO_4$, 0.5% β-mercaptoethanol in PBS). Total SRF activation was calculated by measuring luciferase luminescence using a LMAX II plate reader (Molecular Devices) and corrected for transfection efficiency by measuring β-Galactosidase (β-Gal) absorbance at OD_{594} using a SpectraMax M2 plate reader (Molecular Devices). SRF activity was compared to activation of SRF-VP16, which was set to 100%. In some cases, MARK2 inhibition INF1-induced SRF activity was compared to that of INF1 activation alone, which was set to 100%.

2.4 DNA Plasmids

INF1 full length and truncation plasmids were previously generated as EF plink derivatives with myc, Flag, cherry, or YFP tags. MARK2 pDest27 wild-type, kinase dead

(T208D, S212D), dominant negative (T208A, S212A), and constitutively active (D175A) plasmids were obtained from the laboratory of Dr. Robert Screaton. MARK2 was subcloned into pEF vectors in a two-step process using *NcoI-BamHI-XbaI* restriction enzyme cut sites. Serum Response Factor assay plasmids (3DA.Luc, MLV-LacZ) were generated according to *Geneste et al., 2002 and Sotiropoulos et al., 1999*.

2.5 INF1 Point Mutant Generation

INF1 point mutants (Table 2.2) were generated using a PCR overlap-extension protocol, as explained in *Ho et al., 1989*. Briefly, a short fragment of INF1 that contained the region to be mutated was cut out of the full length DNA fragment. Primers containing a base substitution were used to generate overlapping DNA fragments by PCR. The two resulting fragments were combined into a third PCR and the complementary 3' ends containing the mutation, mutually annealed and served as primers for extension of the complete strand. This fragment of DNA was then re-inserted into the full length INF1 fragment.

Table 2.2: INF1 Point Mutants

S866A	S879A
S866D	S879D
S866A/S879A	S866D/S879D
S1007A	S1034A
S1007D	S1034D

2.6 Statistical Analysis

Microsoft Office Excel and GraphPad Pro software were used for statistical calculations. Data were expressed as means ± standard error of the mean (SEM). Data differences were statistically significant if $P<0.05$ after performing a Student's t-test.

Chapter 3: Results Part I

3.1 INF1 and the Actin Cytoskeleton

INF1 does not possess any previously described regulatory domains. Since INF1 has functional similarities to MAPs and since MAPs are regulated by phosphorylation, we looked at potential kinase inhibitors as INF1 regulators. In addition, preliminary experiments by Kevin Young showed that coexpression of MARK2 inhibited INF1-induced microtubule acetylation.

To determine whether or not INF1 activity is affected by MARK2, we co-expressed the two proteins by transient transfection in NIH-3T3 cells. Overexpression of INF1 induces the formation of actin stress fibers (Figure 3.1.1). Co-expression of wild-type (WT) MARK2 strongly inhibited the ability of INF1 to induce F-actin accumulation while expression of the kinase dead mutant had essentially no effect (Figure 3.1.2). As expected, expression of MARK2 WT, or KD alone, had no effect on actin structure, (Figure 3.1.3).

The immunofluorescence results were confirmed and complemented by Serum Response Factor (SRF) reporter gene assays which indirectly quantify F-actin assembly by measuring G-actin depletion. The SRF reporter gene 3D.A.Luc responds to G-actin depletion and has been shown to be an accurate measure of actin nucleation factor activity (Copeland and Treisman 2002). Transfection of 1.0ug of MARK2 WT significantly inhibited INF1, while KD did not (Figure 3.1.4).

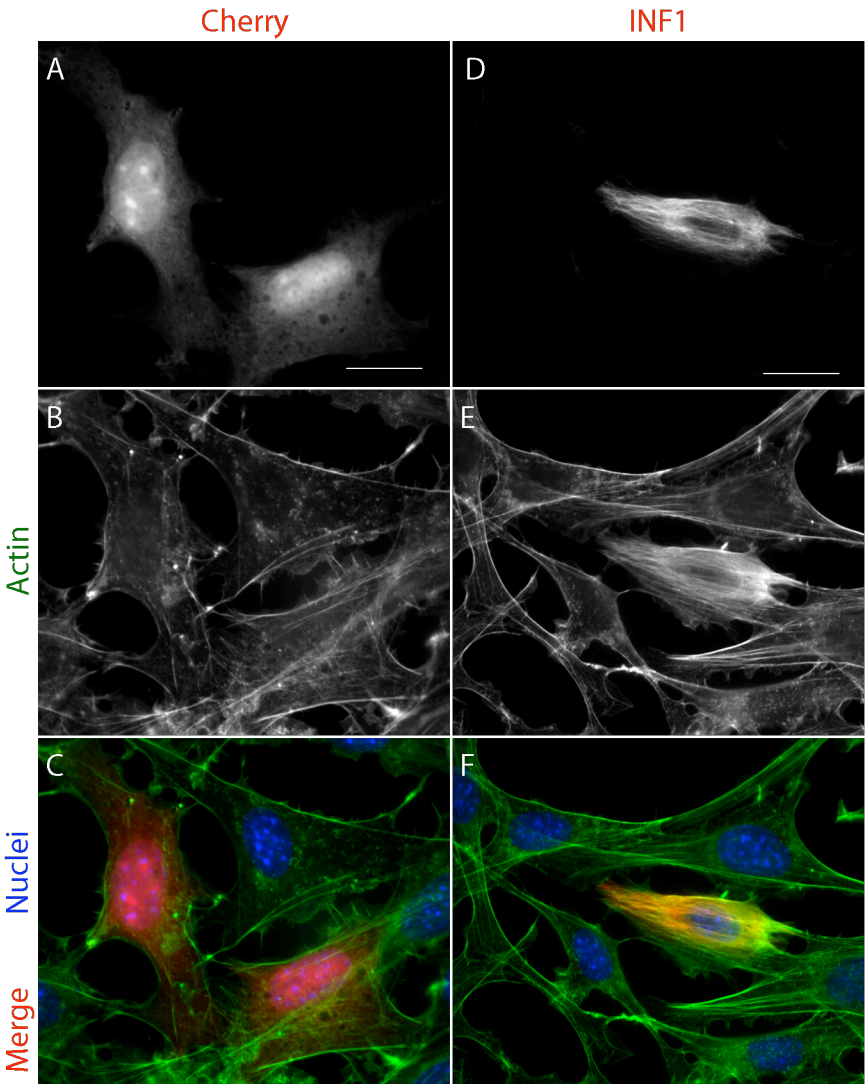

Figure 3.1.1. INF1 induces actin stress fiber formation. Empty cherry-tagged vector (A-C) and cherry-tagged INF1 (D-F) were expressed in NIH-3T3 cells. Cells were transfected and starved in 0.5% DBS DMEM for 24hrs post-transfection, and then fixed in paraformaldehyde. 0.4µg of cherry or INF1 was transfected in each treatment.Scale bar, 20µm.

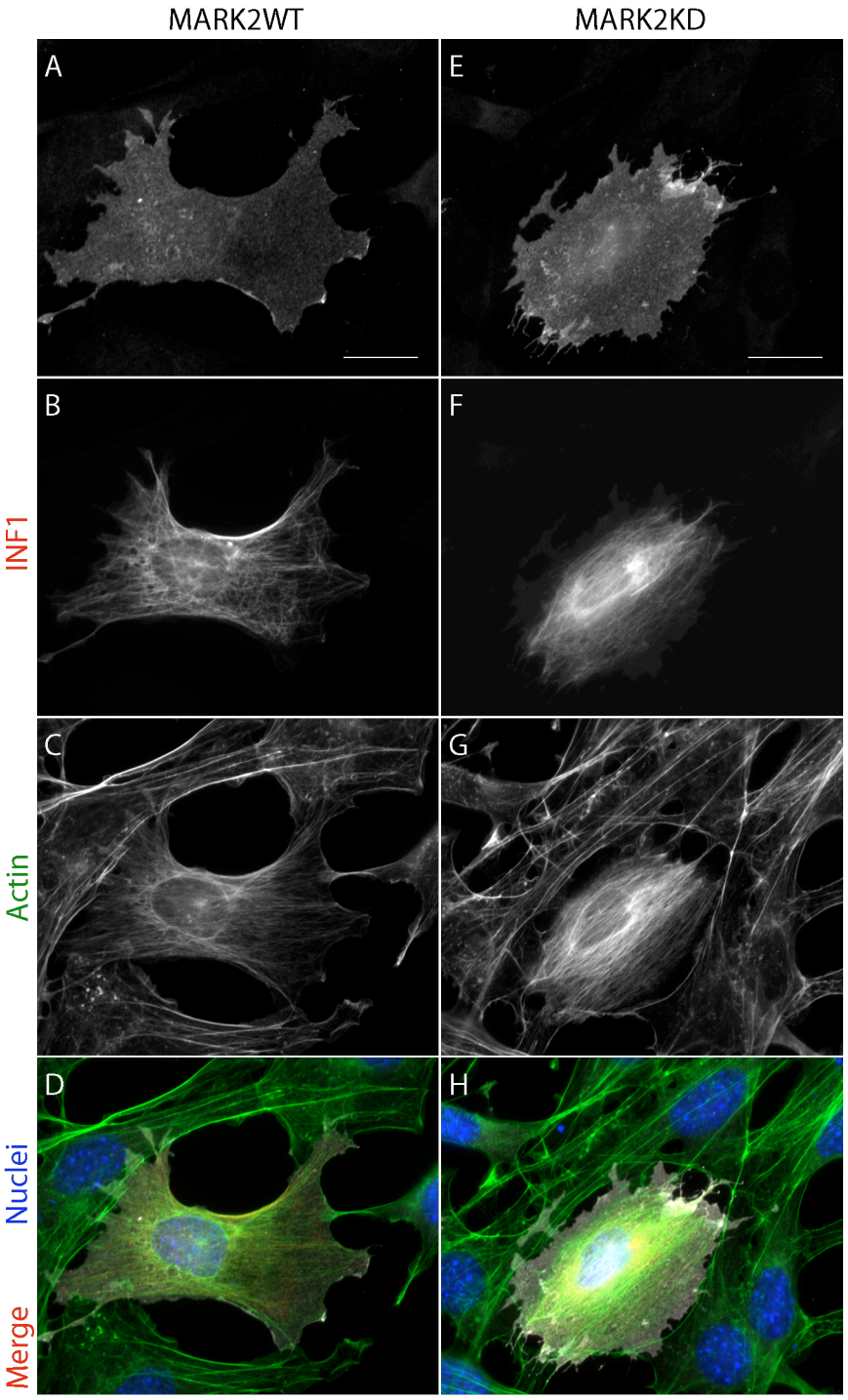

Figure 3.1.2. MARK2 wild type inhibits INF1-induced actin stress fiber formation. Wild-type (A-D) and kinase dead (E-H) MARK2 were coexpressed with cherry-tagged INF1 (A-D). NIH-3T3 cells were transfected and starved n 0.5% DBS DMEM for 24hrs post-transfection, and then fixed in paraformaldehyde. 0.4µg of INF1 and 1.0µg of MARK2 was transfected in each treatment. Scale bar, 20µm.

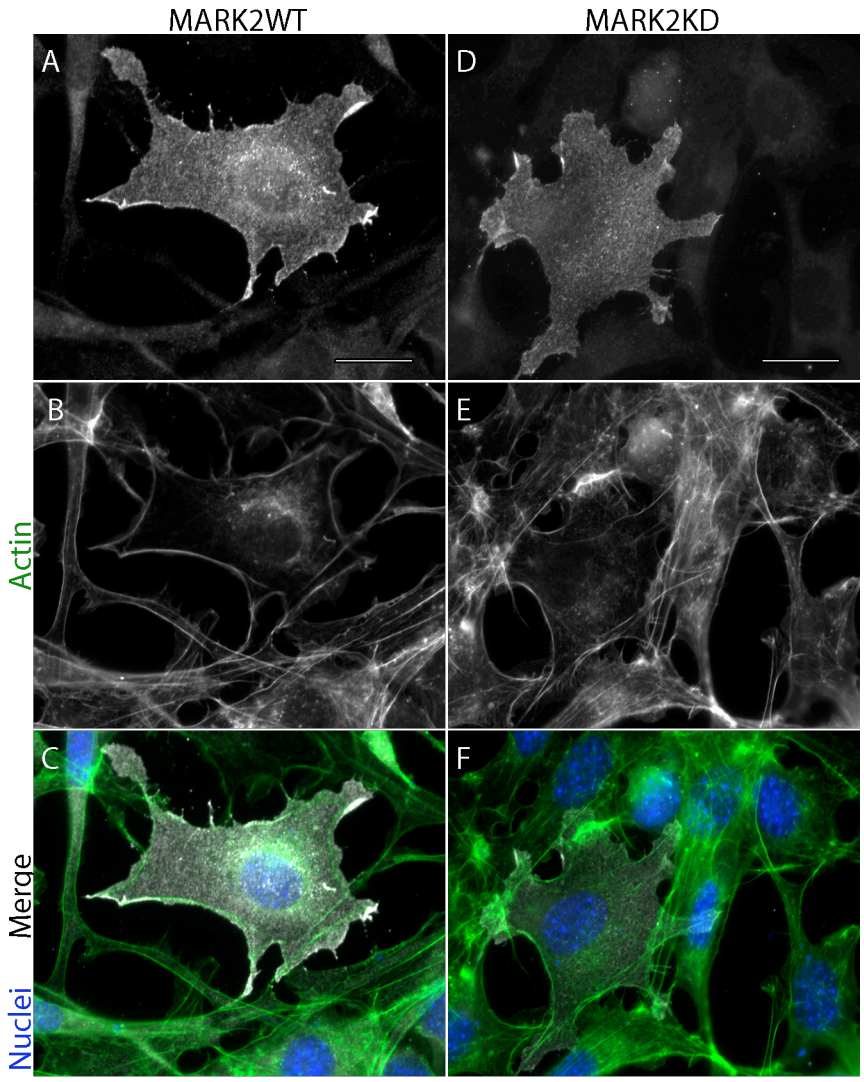

Figure 3.1.3. Expression of MARK2 has no effect on actin. NIH-3T3 cells were transfected with MARK2 wild-type (A-C) or kinase dead (D-F) and starved n 0.5% DBS DMEM for 24hrs post-transfection, and then fixed in paraformaldehyde. 1.0µg of MARK2 was transfected in each treatment. Scale bar, 20µm

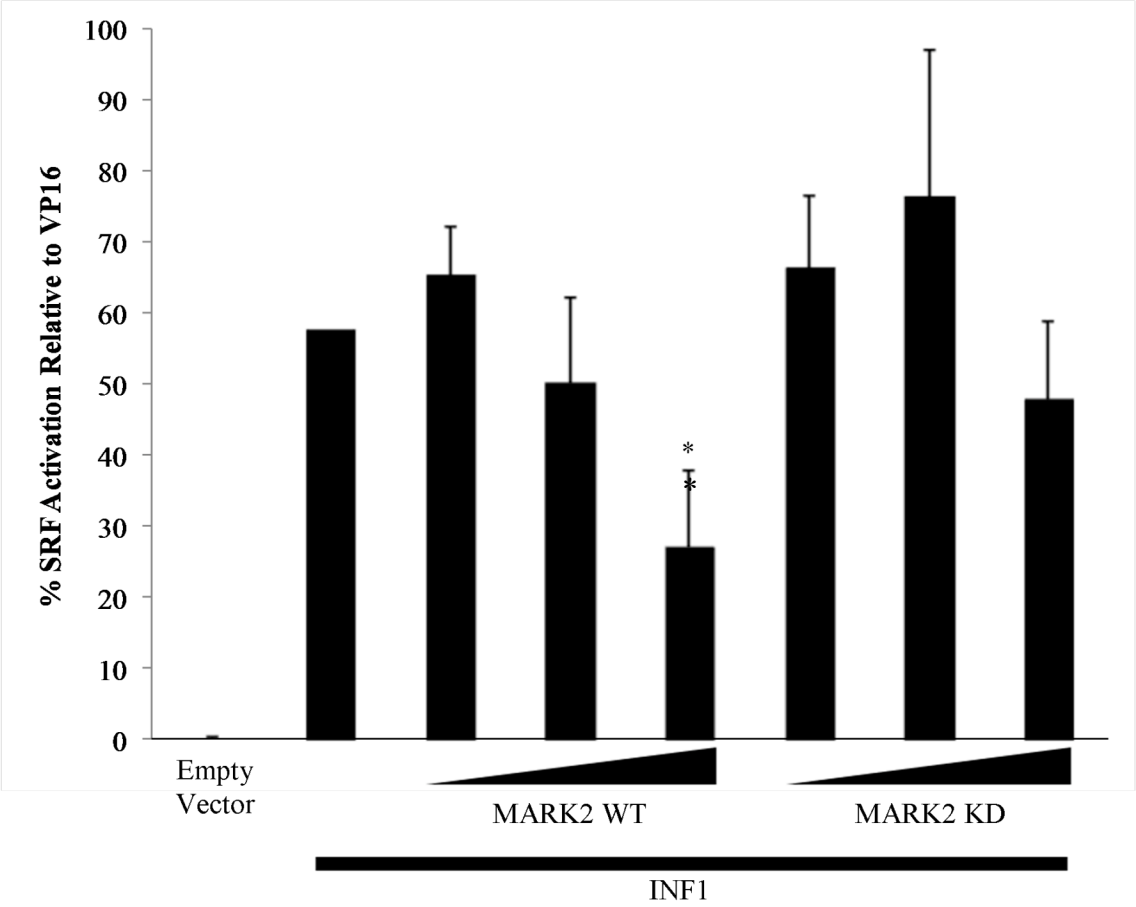

Figure 3.1.4. MARK2 inhibits INF1-induced SRF-activation. Coexpression of MARK2 wild-type inhibits INF1-induced SRF activation. NIH-3T3 cells were starved in 0.5% DBS DMEM for 24 hrs post-transfection, and then lysed in reporter lysis buffer. Activation of SRF is normalized to INF1 at 100%. 0.4µg of INF1 and 0.1, 0.3, or 1.0µg of MARK2 were transfected in each treatment. N=3. * indicates statistical significance compared to INF1.

Since MARK2 was able to inhibit INF1-induced stress fiber formation and SRF activation, we proceeded to determine at which region INF1 was being targeted by MARK2. We used a cherry-FP INF1 1-485 plasmid, which encoded the first 485 amino acids. This fragment is able to induce F-actin accumulation, activate SRF, and induce microtubule acetylation. INF1 1-485 was expressed alone, or with MARK2 WT and KD. Stress fiber formation induced by INF1 1-485 was not inhibited my MARK2 WT, nor was activation of the SRF pathway (Figures 3.1.5 and 3.1.6).

Taken together with the results of INF1 full length inhibition by MARK2, these results indicate that MARK2 inhibited INF1-induced stress fiber formation at the C-terminus of INF1. There are two MARK2 consensus K-X-G-S phosphorylation sites, at S866 and S879 of INF1 (Figure 3.1.7). INF1 also has many K-X-X-S and R-X-X-S sites. INF1 point mutants were created to determine whether INF1 is regulated by phosphorylation at particular K-X-G-S sites. Expression of unphosphorylatable (S866A, S879A, S1007A, and S1034A) and phosphomimetic (S866D, S879D, S1007D, and S1034D) mutants showed no difference in stress fiber formation (Figures 3.1.8 and 3.1.9). SRF activation was also not affected by most point mutations, although activation of SRF by INF1 S879A was significantly reduced compared to wild-type INF1 (Figure 3.1.10).

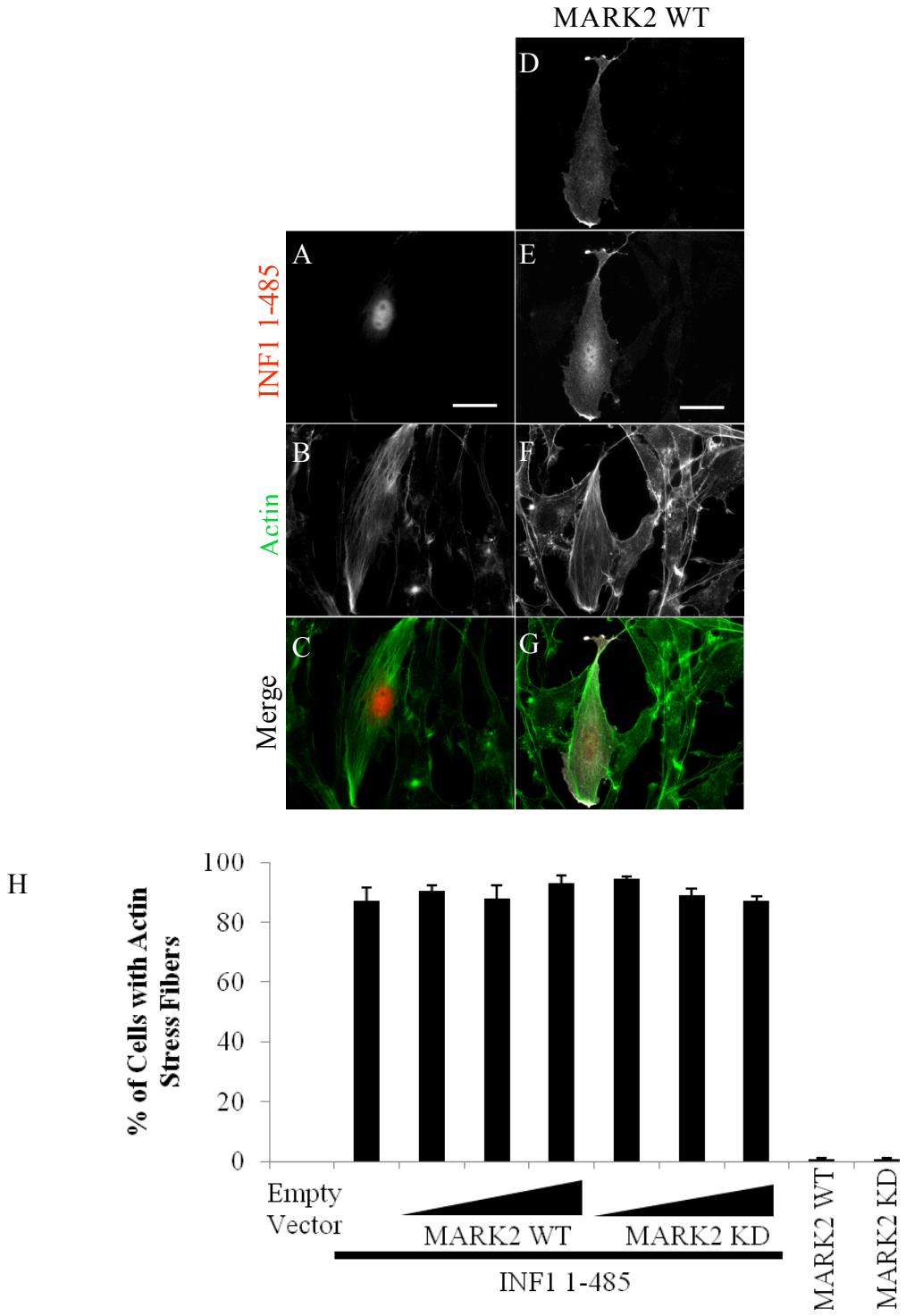

Figure 3.1.5. MARK2 fails to inhibit INF1 1-485-induced actin stress fibers. Cherry-tagged INF1 was expressed alone (A-C) or with MARK2 WT (D-G) in NIH-3T3 cells. Cells were transfected and grown in 0.5% DBS DMEM for 24hrs post-transfection, and then fixed in paraformaldehyde. 0.5µg of INF1 1-485 and 0.5, 0.8, or 1.0µg of MARK2 were transfected. Photo shows a 1.0µg MARK2 transfection. >30 cells were counter in each repeat. N=3. Error bars are +SEM. Scale bar, 20µm.

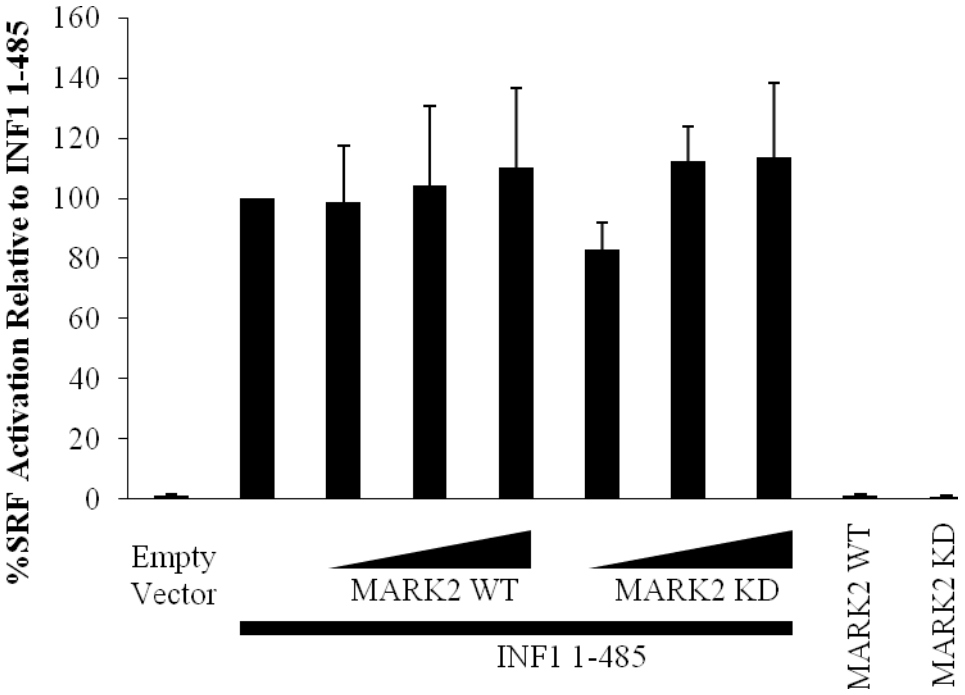

Figure 3.1.6. MARK2 does not inhibit INF1 1-485-induced SRF-activation. INF1 1-485 was expressed with MARK2 wild-type or kinase dead in NIH-3T3 cells. Cells were starved in 0.5% DBS DMEM for 24 post-transfection, and then lysed in reporter lysis buffer. 0.5µg of INF1 1-485 and 0.5, 0.8, or 1.0µg of MARK2 were transfected in each treatment. N=3. Error bars are +SEM.

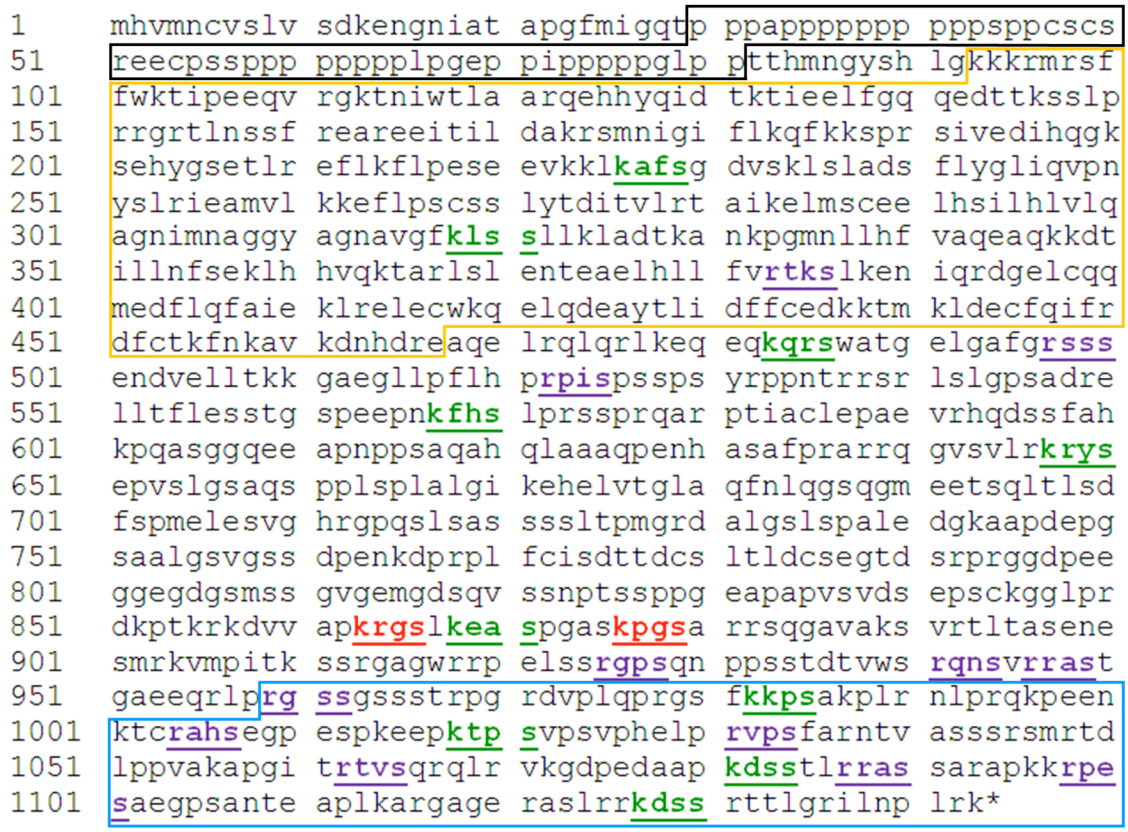

FH1
FH2
MTBD
MARK2 K-X-G-S sites
MARK2 K-X-X-S sites
MARK2 R-X-X-S sites

Figure 3.1.7. INF1 has many MARK2 consensus phosphorylation sites. INF1 point mutants were created for the two K-X-G-S MARK2 consensus sites, as well as the two R-X-X-S sites, located in the microtubule binding domain (MTBD).

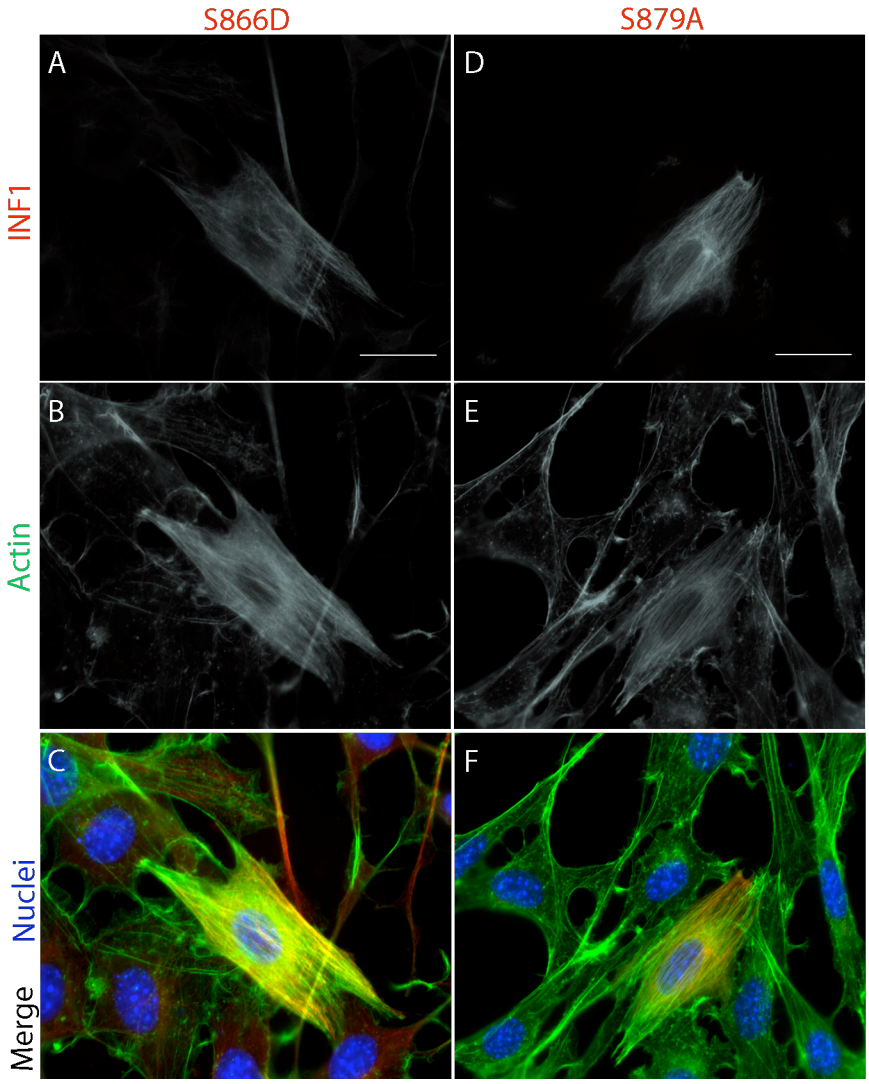

Figure 3.1.8. INF1 point mutants retain the stress-fiber phenotype. Myc-tagged INF1 point mutants were expressed in NIH-3T3 cells. Cells were starved in 0.5% DBS DMEM for 24hrs post-transfection, and then fixed in paraformaldehyde for phenotypic quantification through immunofluorescence imaging. 0.5µg of INF1 mutants were transfected. Scale bar, 20µm.

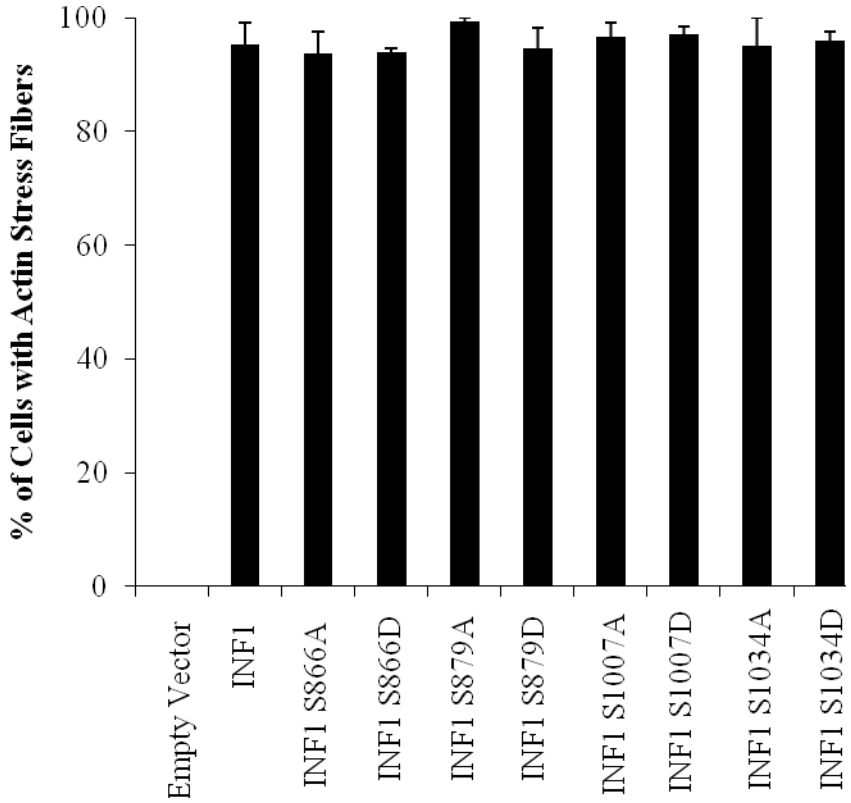

Figure 3.1.9. INF1 point mutants retain the stress-fiber phenotype, part II. NIH-3T3 cells were starved in 0.5% DBS DMEM for 24hrs post-transfection, and then fixed in paraformaldehyde for phenotypic quantification through immunofluorescence imaging. 0.5µg of INF1 mutants were transfected. >50 cells were counted for each repeat. N=3.

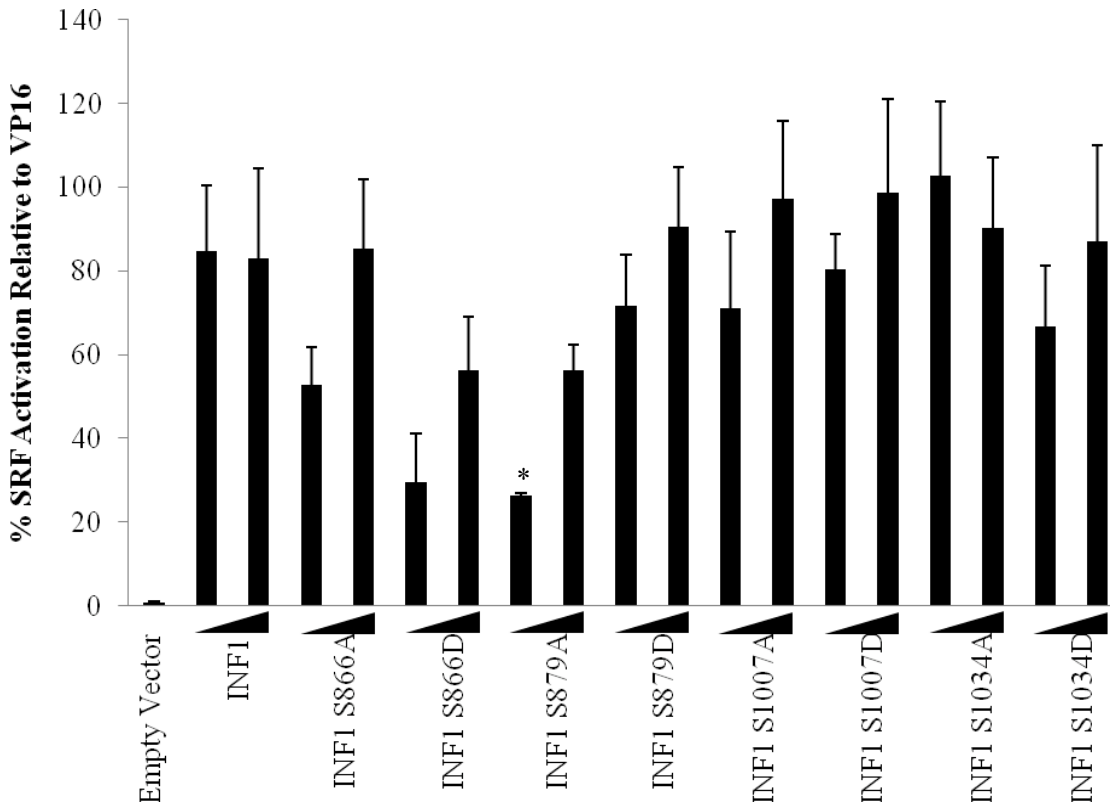

Figure 3.1.10. INF1 point mutants retain the ability to activate SRF. NIH-3T3 cells were starved in 0.5% DBS DMEM for 24hrs post-transfection, and then lysed in reporter lysis buffer. Two concentrations of each plasmid were used. 0.3 or 0.7µg of each construct was transfected. * indicates statistical significance between 0.3µg INF1 S879A and 0.3µg INF1 WT.

3.2 INF1 and Microtubules

INF1 induces microtubule stabilization and acetylation. Preliminary data suggested that MARK2 inhibits INF1-induced microtubule-acetylation in NIH-3T3 cells. MARK2 was coexpressed with INF1 in NIH-3T3 cells to determine its ability to inhibit INF1-induced microtubule acetylation. However, co-expression of MARK2 failed to inhibit INF1's ability to induce acetylated microtubule formation in NIH-3T3 cells (Figures 3.2.1-3.2.4). Further, we looked at whether MARK2 could inhibit INF1's N-terminus acetylation activity by coexpressing INF1 1-485 with MARK2. In this case, MARK2 failed to inhibit INF1's ability to induce microtubule acetylation (Figure 3.2.5).

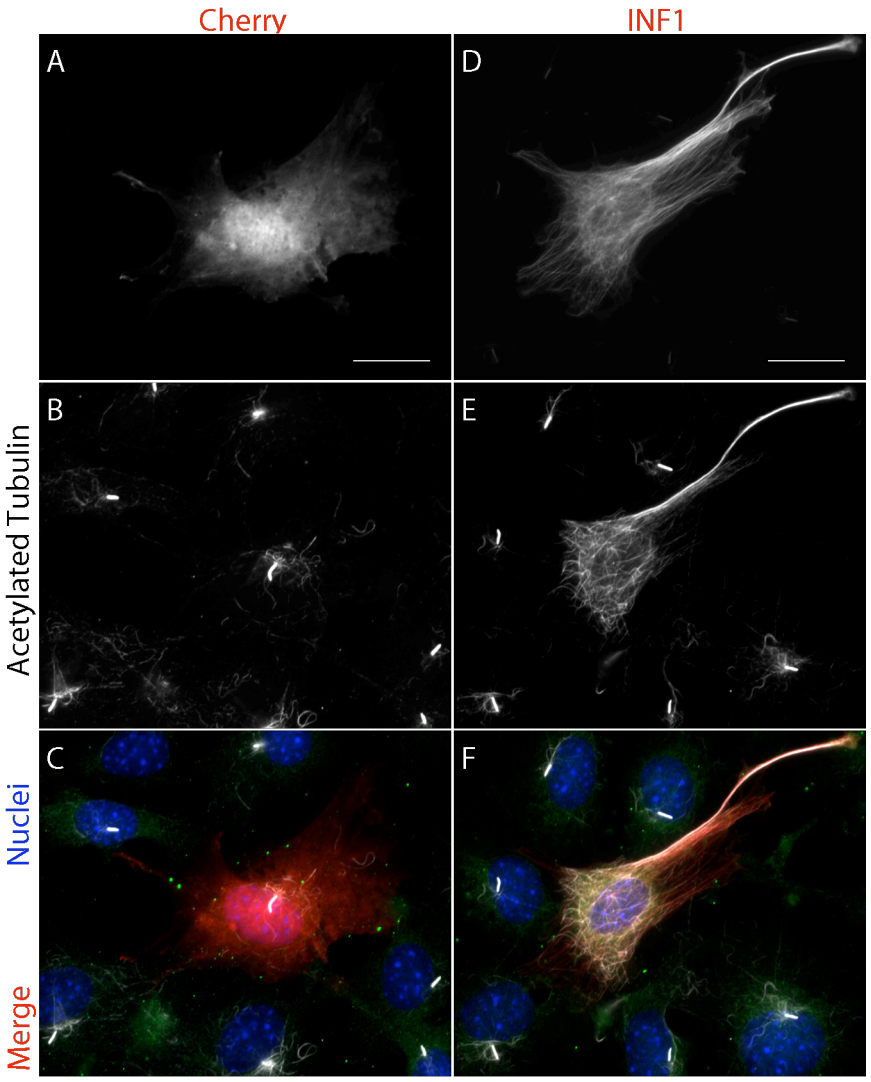

Figure 3.2.1. INF1 induces microtubule acetylation. Empty cherry-tagged vector (A-C) and cherry-tagged INF1 (D-F) were expressed in NIH-3T3 cells. Cells were transfected and starved in 0.5% DBS DMEM for 48hrs post-transfection, and then fixed in paraformaldehyde. Thick acetylated tubulin projections in the perinuclear region are primary cilia. 0.4µg of cherry or INF1 was transfected. Scale bar, 20µm.

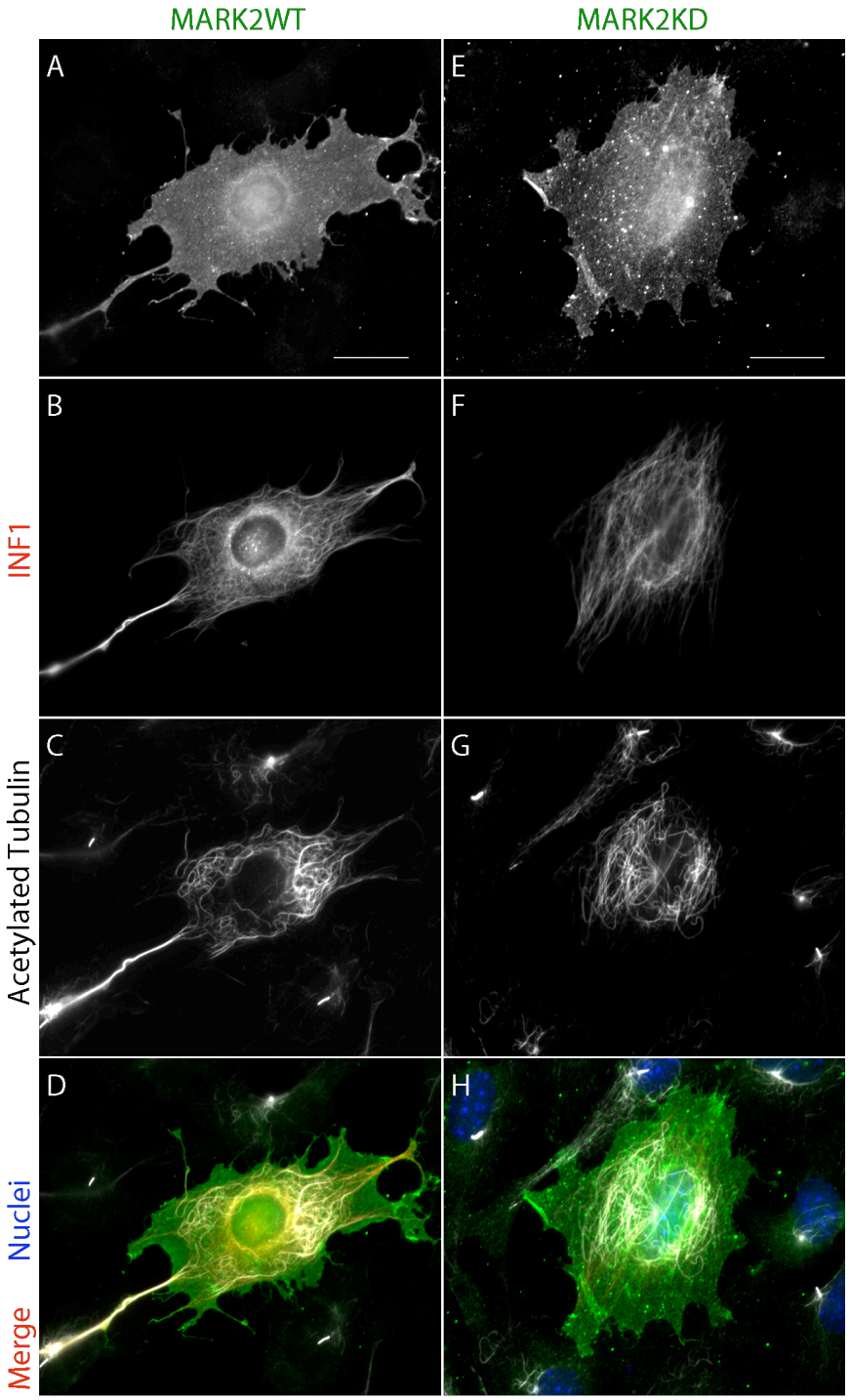

Figure 3.2.2. MARK2 does not inhibit INF1-induced microtubule acetylation. Wild-type (A-D) and kinase dead (E-H) MARK2 were coexpressed with cherry-tagged INF1. NIH-3T3 cells were transfected and starved in 0.5% DBS DMEM for 48hrs post-transfection, and then fixed in paraformaldehyde. 0.2µg of INF1 and 1.3µg of MARK2 were transfected in each treatment. Scale bar, 20µm.

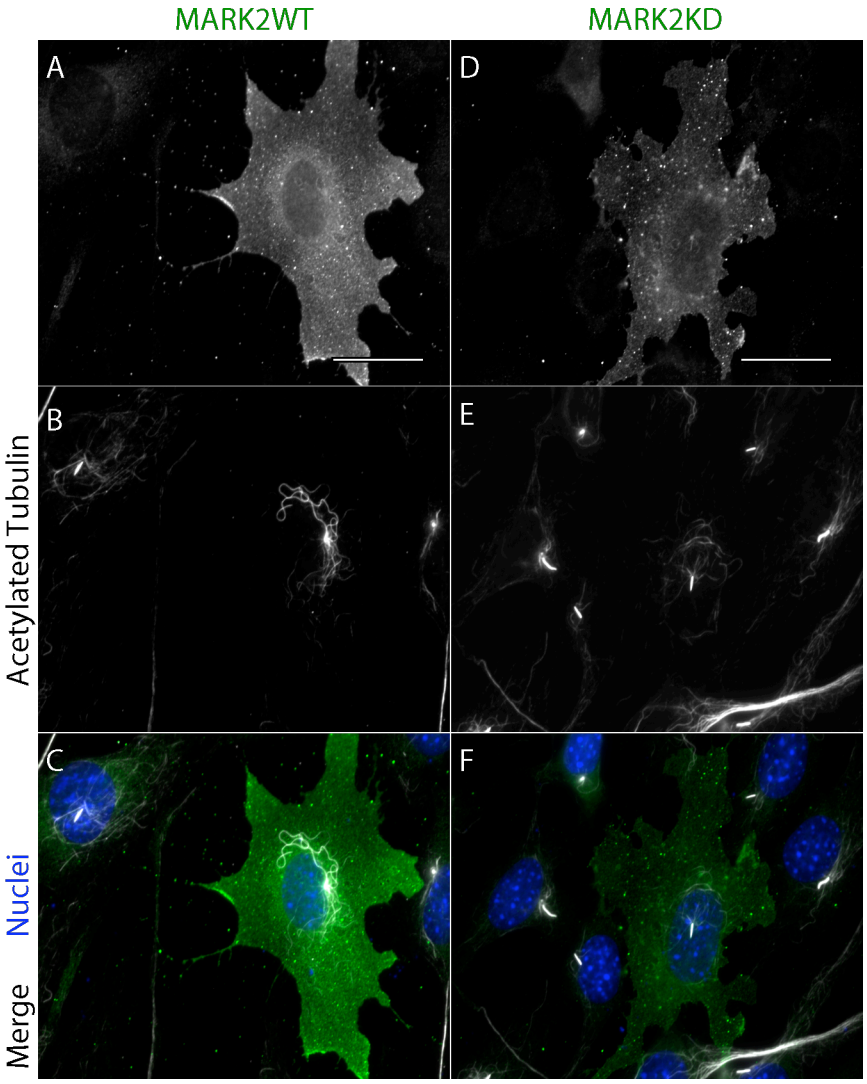

Figure 3.2.3. Expression of MARK2 has no effect on microtubule acetylation. NIH-3T3 cells were transfected with MARK2 wild-type (A-C) or kinase dead (D-F) and starved in 0.5% DBS DMEM for 48hrs post-transfection, and then fixed in paraformaldehyde. 1.3µg of MARK2 was transfected in each treatment. Scale bar, 20µm.

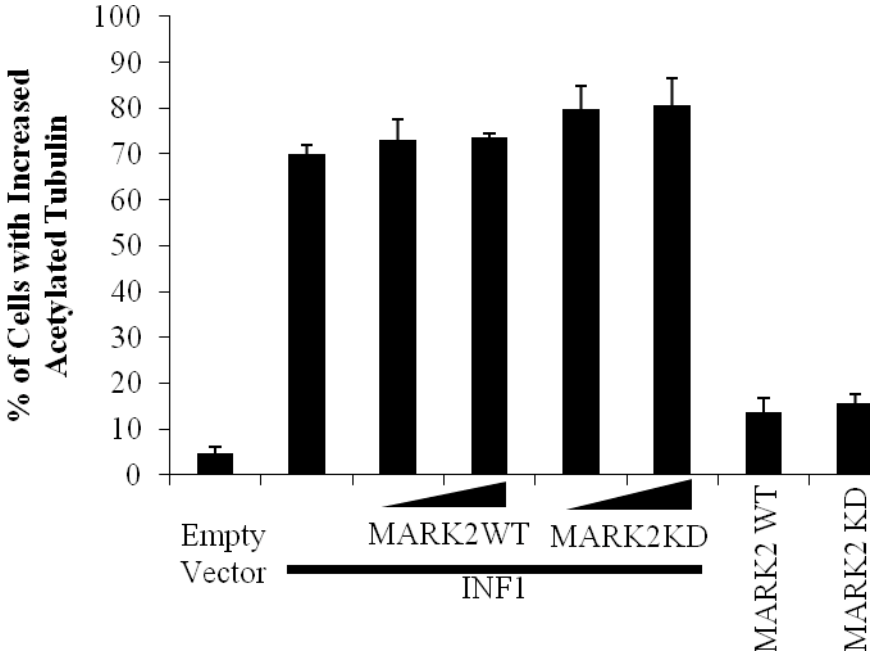

Figure 3.2.4. MARK2 has no effect on INF1-induced microtubule acetylation. NIH-3T3 cells were starved in 0.5% DBS DMEM for 48hrs post-transfection, and then fixed in paraformaldehyde. 0.2µg of INF1 and 0.7 or 1.0µg of MARK2 was transfected in each treatment. >30 cells counted per repeat. N=3.

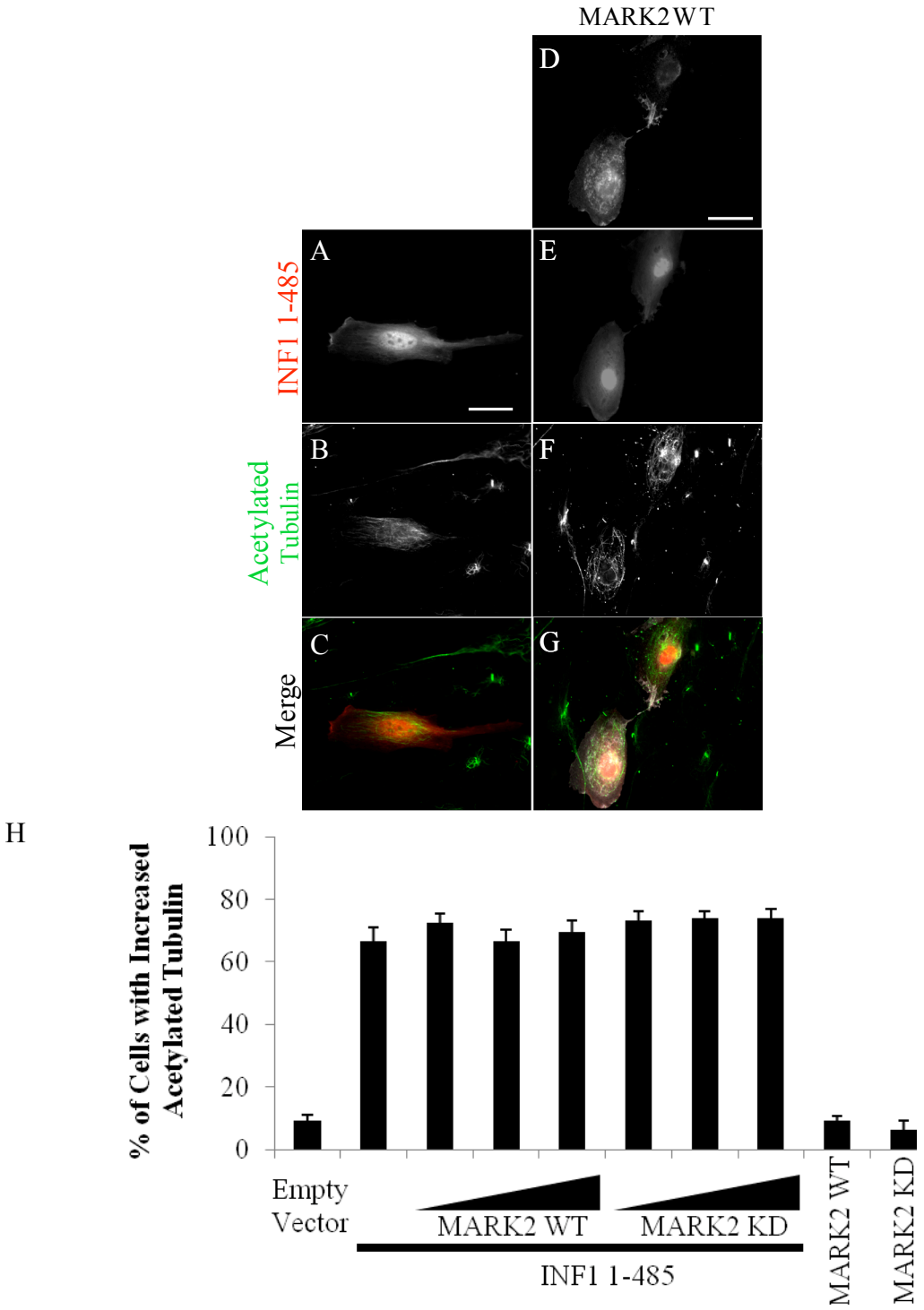

Figure 3.2.5. INF1 1-485 induces microtubule acetylation. Cherry-tagged INF1 was expressed alone (A-C) or with MARK2 WT (D-G) in NIH-3T3 cells. Cells were transfected and grown in 0.5% DBS DMEM for 48hrs post-transfection, and then fixed in paraformaldehyde. 0.4µg of INF1 1-485 and 0.1, 0.3, or 1.0µg of MARK2 were transfected in each treatment. >30 cells counted for each repeat. N=3. Scale bar, 20µm.

INF1 forms an association with microtubules through its C-terminal microtubule binding domain (MTBD). Phosphorylation by MARK2 has been shown to inhibit microtubule binding of a number of MAPs (Ebneth and Mandelkow, 1999). Thus we wished to determine if co-expression of MARK2 interfered with the ability of INF1 to colocalize with microtubules. MARK2 was coexpressed with INF1 in NIH-3T3 cells by transient transfection and the effect on INF1 subcellular localization was assessed by immunofluorescence. In these experiments the co-expression of MARK2 did not have any obvious effect on the ability of INF1 to associate with the MT network (Figures 3.2.6 and 3.2.7).

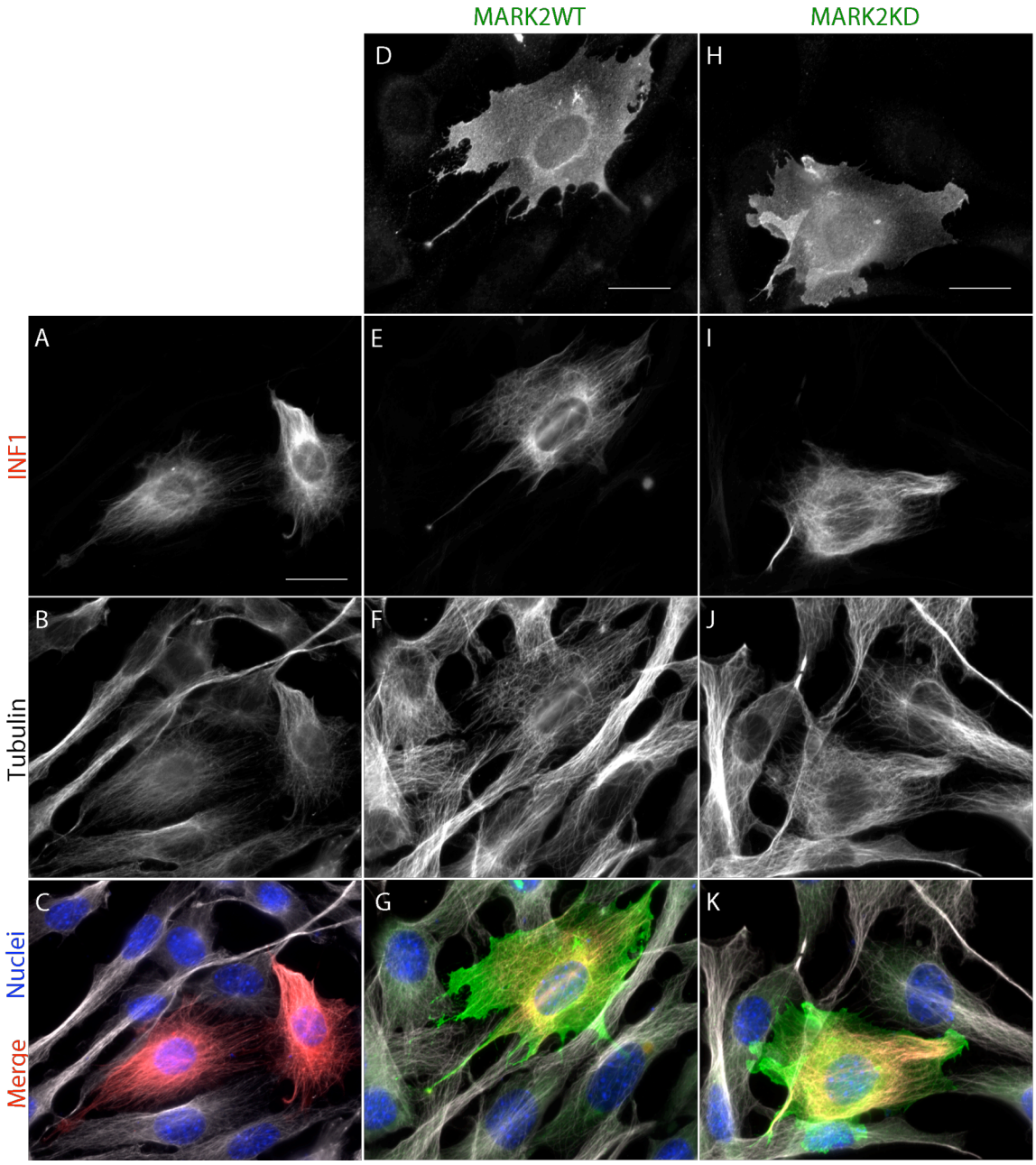

Figure 3.2.6. MARK2 does not inhibit INF1 colocalization with microtubules. Cherry-tagged INF1 was expressed alone (A-C), with wild-type (D-G) and kinase dead (H-K) MARK2. NIH-3T3 cells were transfected and grown in 10% DBS DMEM for 24hrs post-transfection, and then fixed in paraformaldehyde. 0.2µg of INF1 and 1.3µg of MARK2 were transfected in each treatment. INF1 is indicated in red and tubulin is indicated in white on merged image. Scale bar, 20µm.

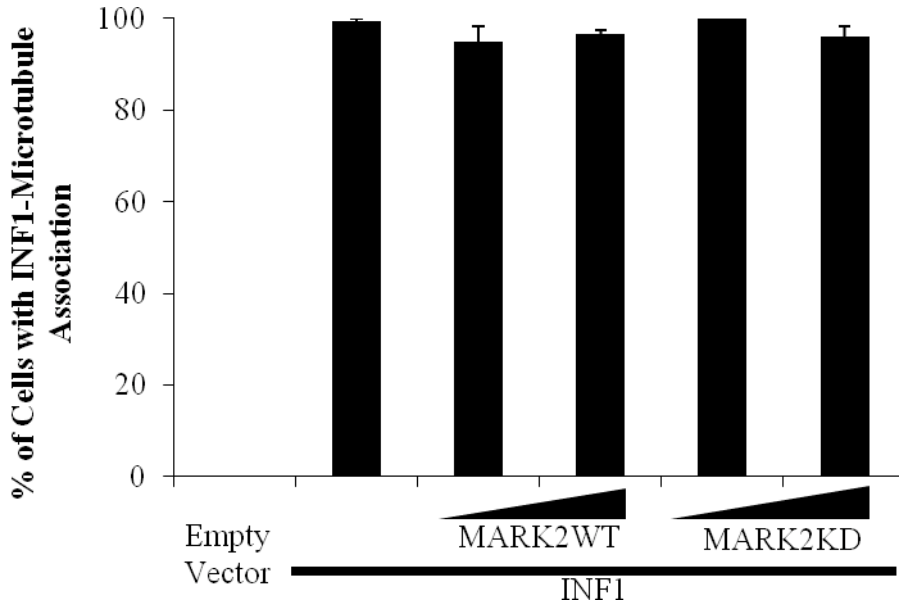

Figure 3.2.7. MARK2 does not inhibit INF1-microtubule colocalization. NIH-3T3 cells were transfected and grown in 10% DBS DMEM for 24hrs post-transfection, and then fixed in paraformaldehyde. 0.2μg of INF1 and 0.7 or 1.3. >30 cells were counted for each repeat. N=3.

3.3 INF1 and Golgi Dispersion

Previously, our lab has showed that endogenous INF1 localizes to the perinuclear region of the leading edges of migrating cells. Co-staining for Golgi markers revealed an association of endogenous INF1 with the Golgi in motile cells. Overexpression of INF1 in NIH-3T3 cells also disperses the Golgi from a polarized location in the perinuclear region and into mini-stacks, which retain their ability to traffic protein.

MARK2 was coexpressed with INF1 in NIH-3T3 cells in order to determine whether INF1-induced Golgi dispersion may be inhibited. Consistent with actin stress fiber formation, microtubule acetylation, and microtubule affinity, INF1's ability to disperse the Golgi was unaffected by the coexpression of MARK2 (Figures 3.3.1-3.3.4).

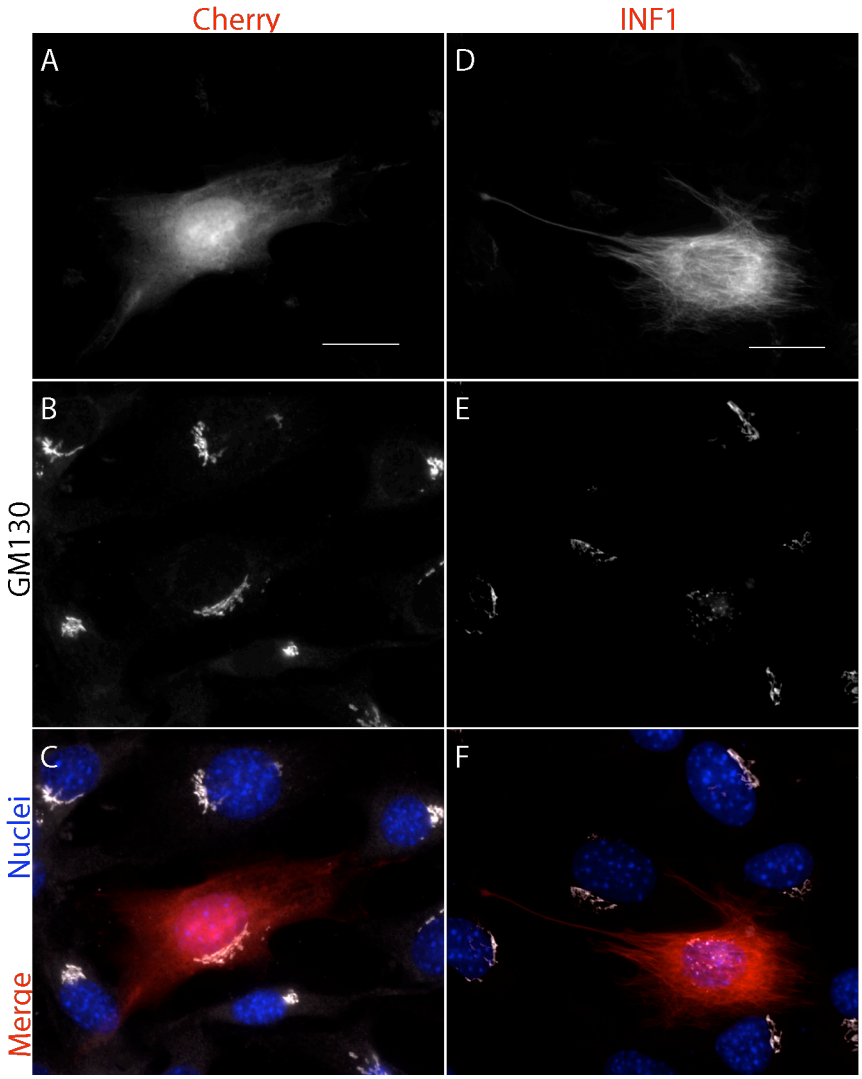

Figure 3.3.1. INF1 induces Golgi dispersion. Empty cherry-tagged vector (A-C) or cherry-tagged INF1 (D-F) were expressed in NIH-3T3 cells. Cells were transfected and grown in 10% DBS DMEM for 24 post-transfection, and then fixed in paraformaldehyde. 0.2µg of cherry or INF1 were transfected in each treatment. Scale bar, 20µm. GM130 is a Golgi marker.

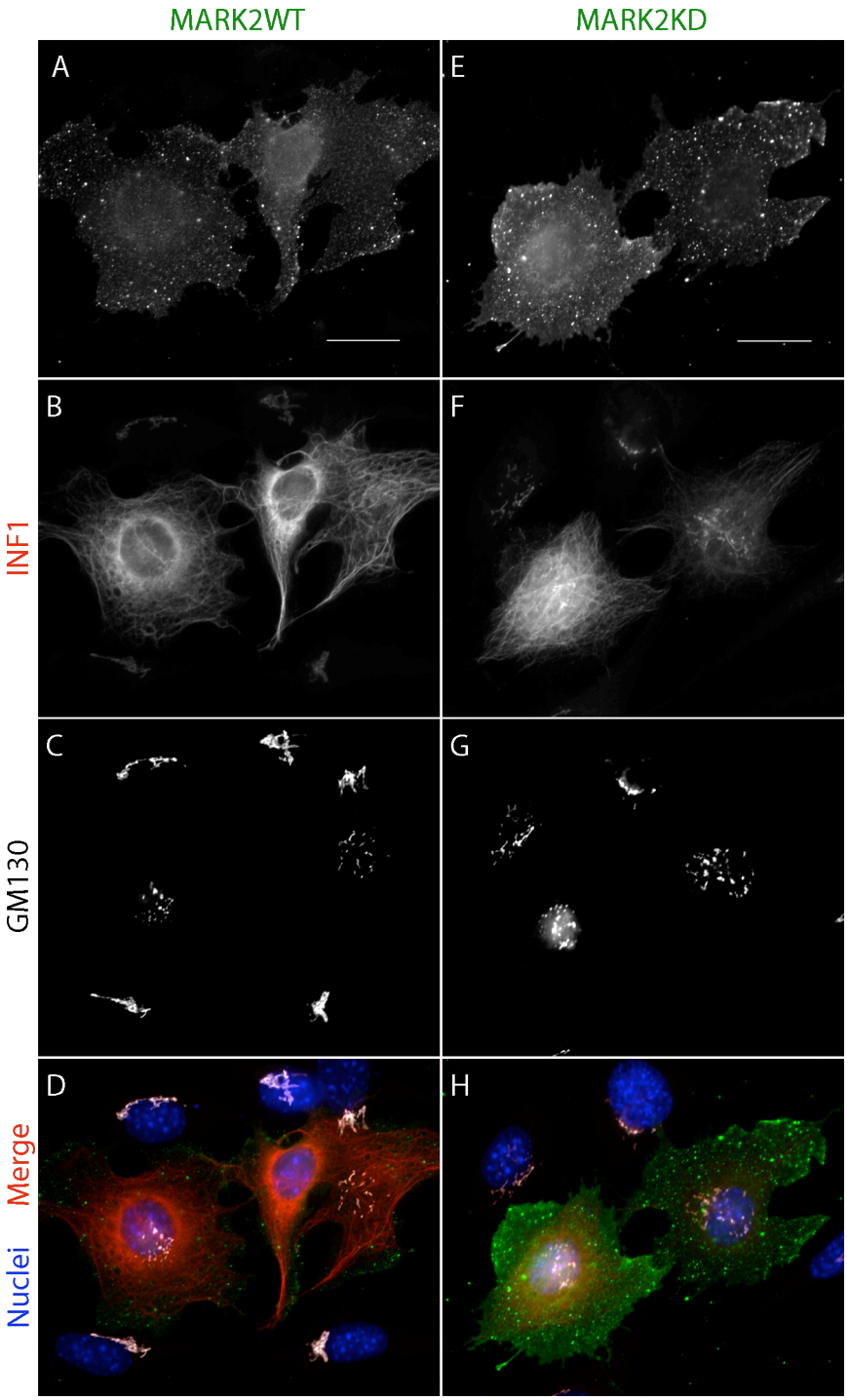

Figure 3.3.2. MARK2 does not inhibit INF1-induced Golgi dispersion. Wild-type MARK2 was coexpressed with INF1 (A-D). Meanwhile, kinase-dead coexpression with INF1 had a similar effect (E-H). NIH-3T3 cells were transfected and grown in 10% DBS DMEM for 24hrs post-transfection, and then fixed in paraformaldehyde. 0.2ug of INF1 and 1.3ug of MARK2 were transfected in each treatment. Scale bar, 20μm. GM130 is a Golgi marker.

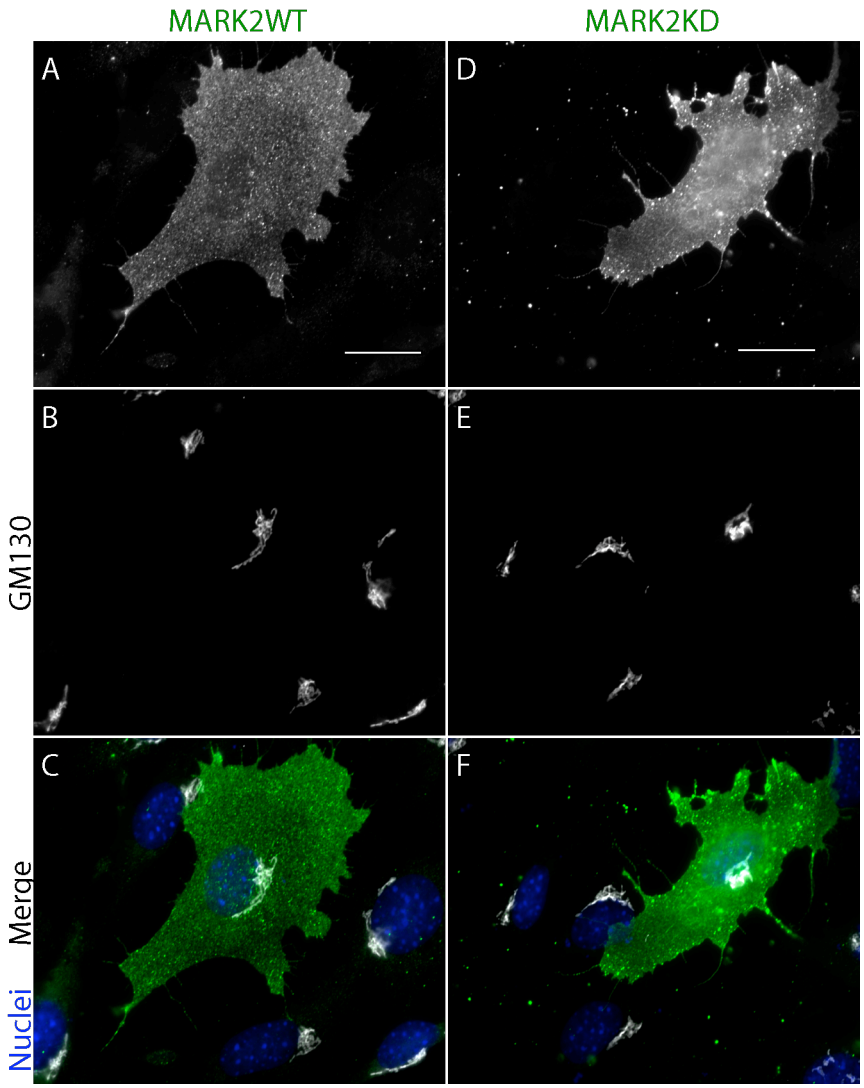

Figure 3.3.3. Expression of MARK2 does not disperse the Golgi ribbon. NIH-3T3 cells were transfected with MARK2 wild-type (A-C) or kinase dead (D-F) and starved in 10% DBS DMEM for 24hrs post-transfection, and then fixed in paraformaldehyde. 1.3ug of MARK2 was transfected in each treatment. GM130 is a Golgi marker. Scale bar, 20µm.

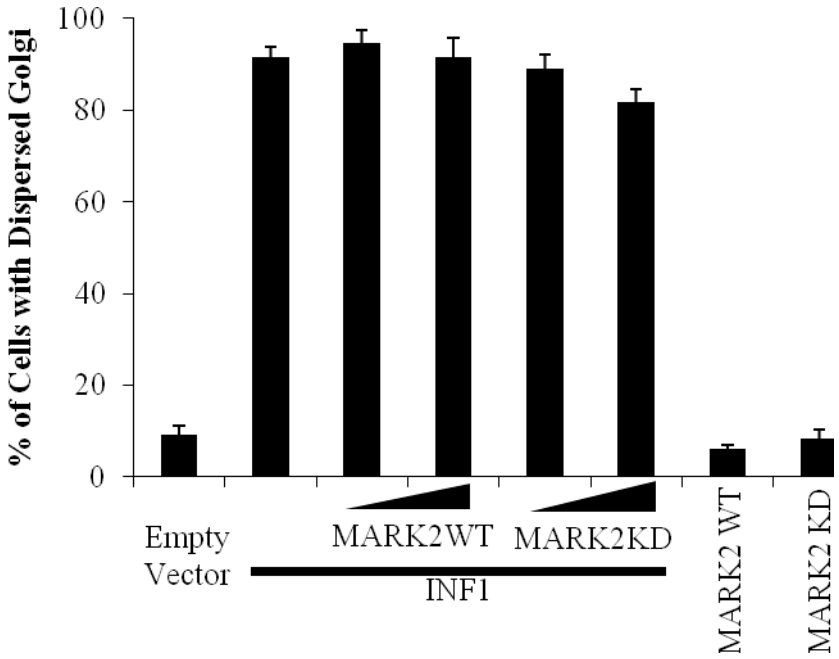

Figure 3.3.4. MARK2 has no effect on INF1-induced Golgi dispersion. NIH-3T3 cells were grown in 10% DBS DMEM for 24hrs post-transfection, and then fixed in paraformaldehyde. 0.2µg of INF1 and 0.7 or 1.3µg of MARK2 were transfected in each treatment. >30 cells were counted in each repeat. N=3.

3.4 INF1 Point Mutants

INF1 point mutants were created to determine whether INF1 is regulated in general by phosphorylation at particular K-X-G-S motifs. Earlier, we showed that expression of many unphosphorylatable and phosphomimetic mutants showed no difference in stress fiber formation and SRF activation (aside from S879A). To complement these results, expression of INF1 point mutants also showed no difference compared to INF1 wild-type in terms of microtubule acetylation, microtubule affinity, and Golgi dispersion (Figures 3.4.1-3.4.4). This data suggests that INF1 is not regulated by phosphorylation at these sites by upstream kinases.

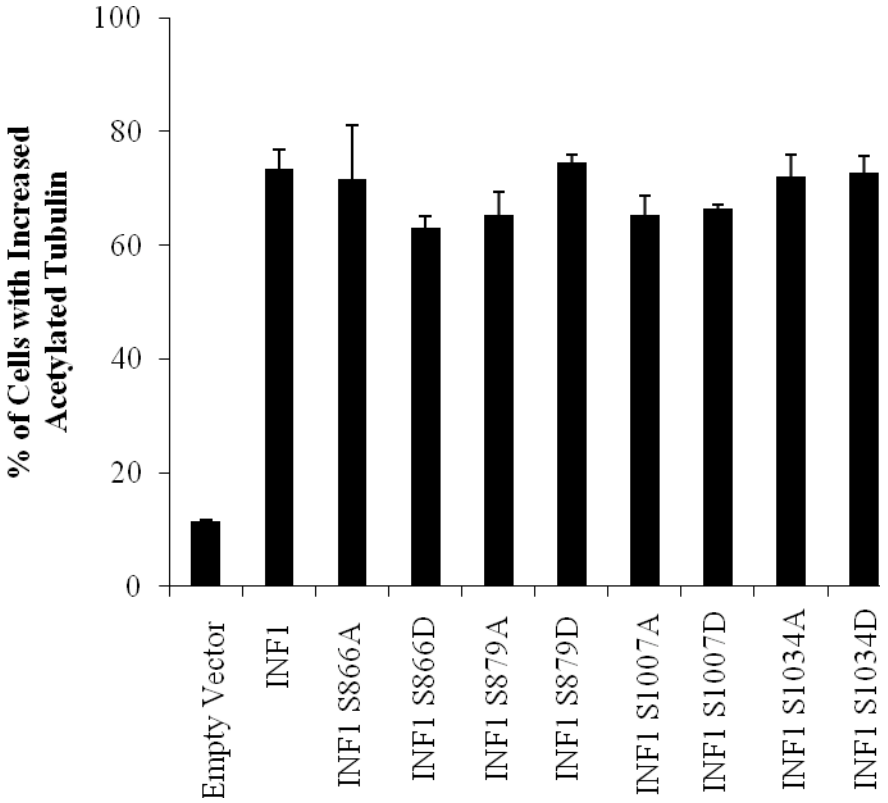

Figure 3.4.1. INF1 point mutants retain the ability to stabilize microtubules. NIH-3T3 cells were starved in 0.5% DBS DMEM for 48hrs post-transfection, and then fixed in paraformaldehyde for phenotypic quantification through immunofluorescence imaging. 0.5ug of relevant INF1 construct was transfected. >50 cells were counted for each repeat. N=3.

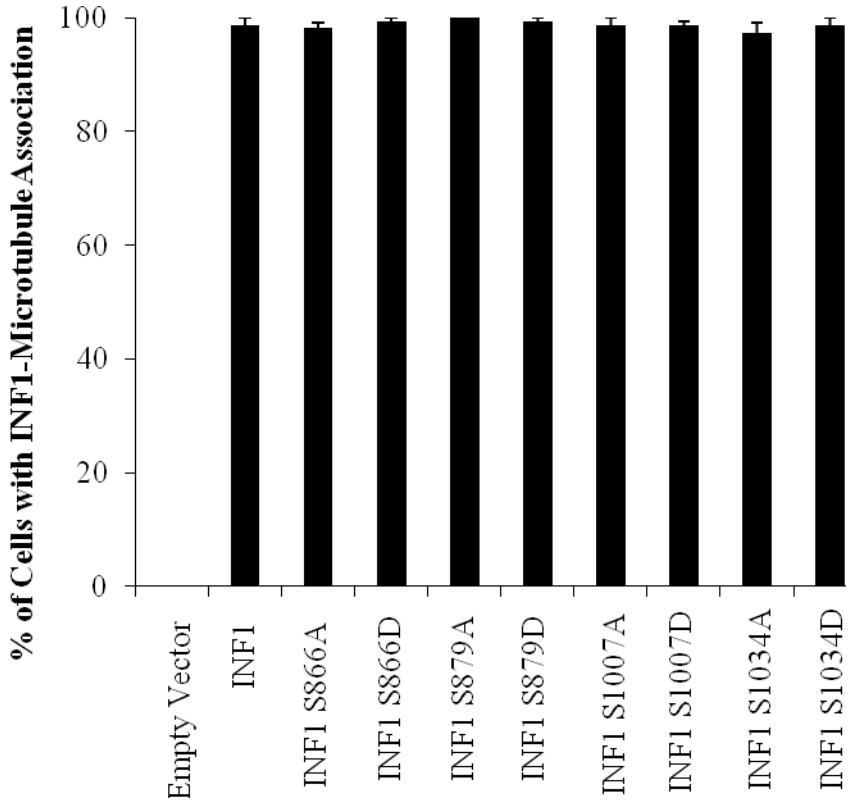

Figure 3.4.2. INF1 point mutants retain the ability to colocalize with microtubules. NIH-3T3 cells were grown in 10% DBS DMEM for 24hrs post-transfection, and then fixed in paraformaldehyde for phenotypic quantification through immunofluorescence imaging. 0.5ug of relevant INF1 construct was transfected. >50 cells were counted for each repeat. N=3.

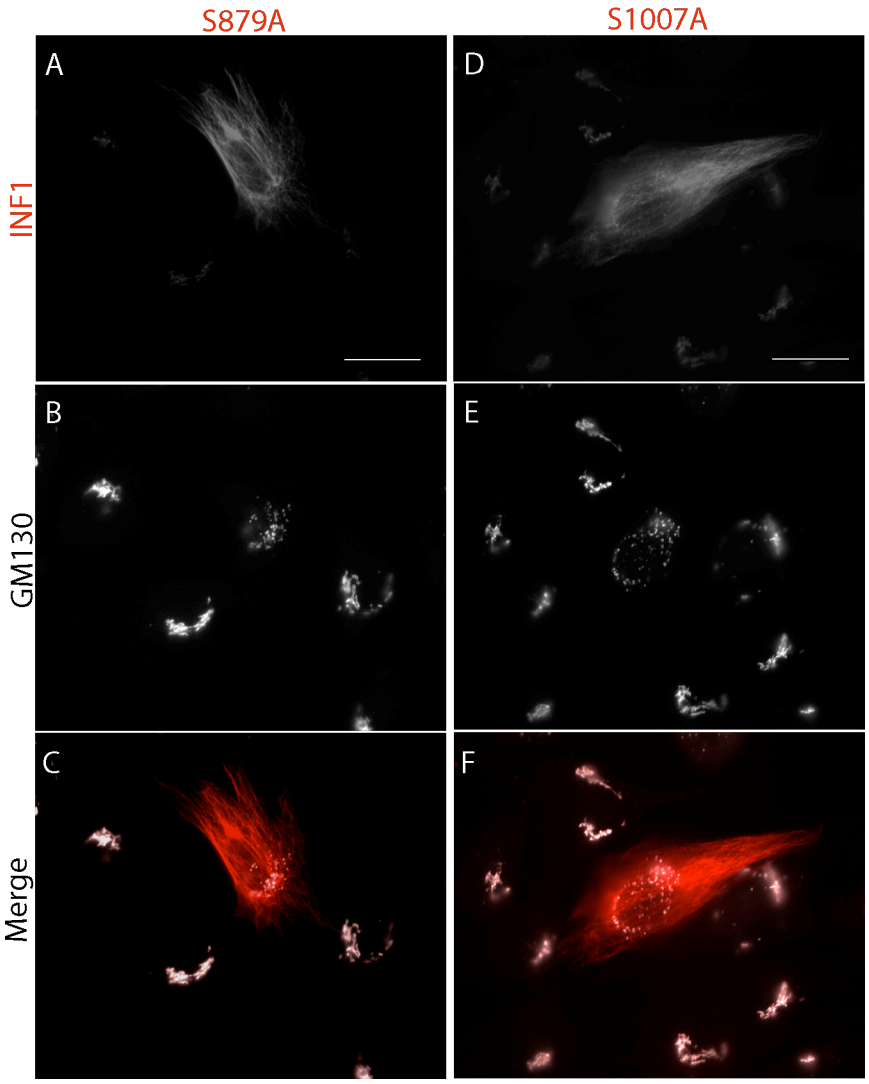

Figure 3.4.3. INF1 point mutants retain the ability to disperse the Golgi ribbon. Myc-tagged INF1 mutants were expressed in NIH-3T3 cells. Golgi body was stained using the Golgi marker GM130. Cells were grown in 10% DBS DMEM for 24hrs post-transfection, and then fixed in paraformaldehyde. 0.5ug of relevant INF1 construct was transfected. Scale bar = 20μm.

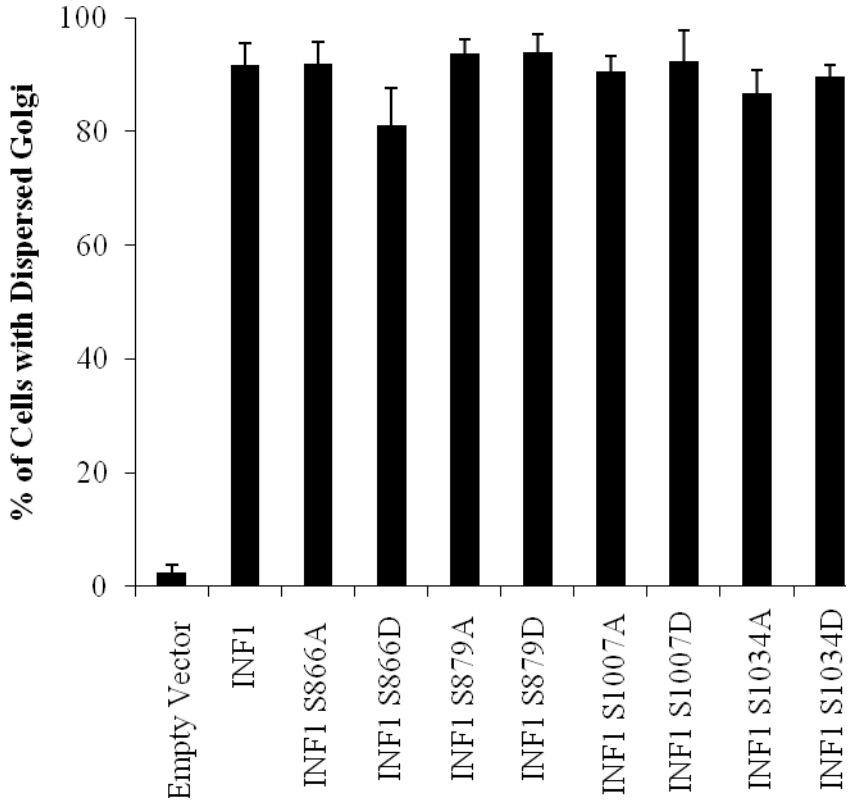

Figure 3.4.4. INF1 point mutants retain the ability to disperse the Golgi ribbon, part II. NIH-3T3 cells were grown in 10% DBS DMEM for 24hrs post-transfection, and then fixed in paraformaldehyde for phenotypic quantification through immunofluorescence imaging. 0.5ug of relevant INF1 construct was transfected. >50 cells were counted for each repeat. N=3.

3.5 INF1 and Cilia

We noted that INF1 overexpression affected cilia in prior experiments looking at acetylated tubulin (Figure 3.2.1). Primary cilia are projections of acetylated tubulin extending out from the perinuclear region of the cell and are involved in numerous sensory mechanisms. Presence of cilia is associated with cells being in G_0, while cilia absence is associated with mitosis, since basal bodies are used as mitotic spindle assembly points (Tucker et al., 1979, Wheatley et al., 1996). Cilia were visualized using an acetylated-tubulin antibody. In cherry-FP expressing cells, cilia were present in 84% of cells. We noted in our initial experiments that overexpression of INF1 is associated with an absence of the primary cilium, (Figures 3.5.1 and 3.5.2). Only 18% of INF1-expressing cells had primary cilia, while cilia were present in 84% of cells expressing cherry-FP. We next examined the ability of other INF1 derivatives to affect cilia formation. The expression of INF1 I180A and 1-958 also inhibited cilia formation, while INF1 486C expression did not inhibit cilia formation (Figure 3.5.2).

In cherry-expressing cells, cilia length was on average 3.9μm in length. However, in those INF1 expressing cells that had cilia, the cilia were exceptionally long, with an average length of 12.1μm. Similarly, expression of I180A and 486C also induced the growth of overly long cilia. From the limited sample size, it is not clear if 1-958 expression has a similar effect (Figure 3.5.3).

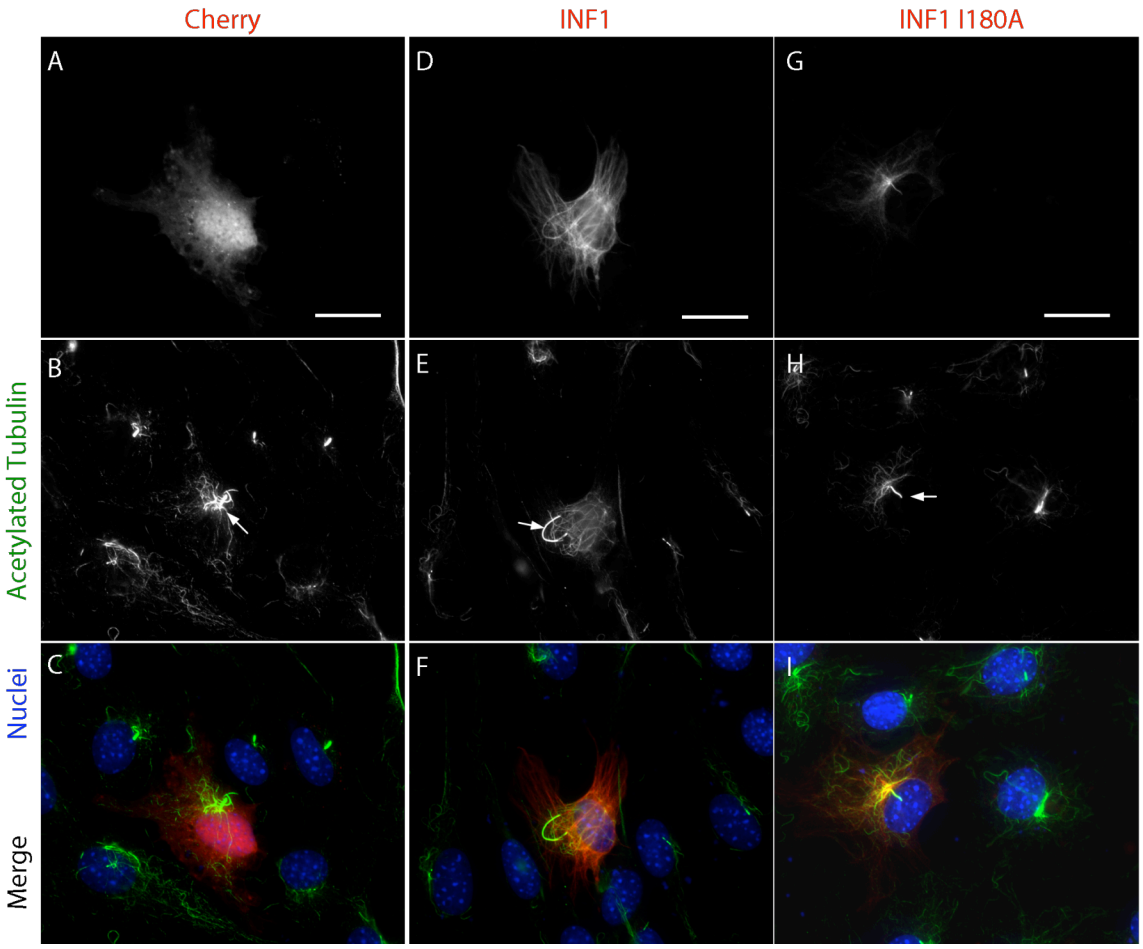

Figure 3.5.1. INF1 overexpression is associated with an elongated cilium in rare cases. INF1 full length and I180A mutant constructs were expressed in NIH-3T3 cells and grown in 0.5% DBS DMEM, then fixed in paraformaldehyde. Primary cilia were detected by an anti-acetylated tubulin antibody. 0.5µg of relevant construct was transfected. Arrows indicate primary cilia. Scale bar, 20µm.

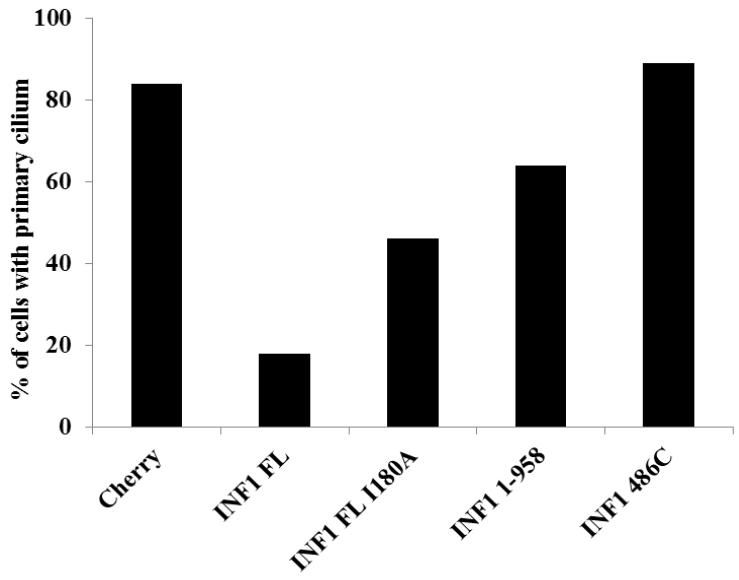

Figure 3.5.2. INF1 overexpression is associated with the absence of primary cilia. INF1 full length and truncation derivatives were expressed in NIH-3T3 cells in 0.5% DBS DMEM and fixed in paraformaldehyde after 48hrs. Primary cilia were detected by an anti-acetylated tubulin antibody. 0.5μg of relevant construct was transfected. 50 cells were counted for each construct. N=1.

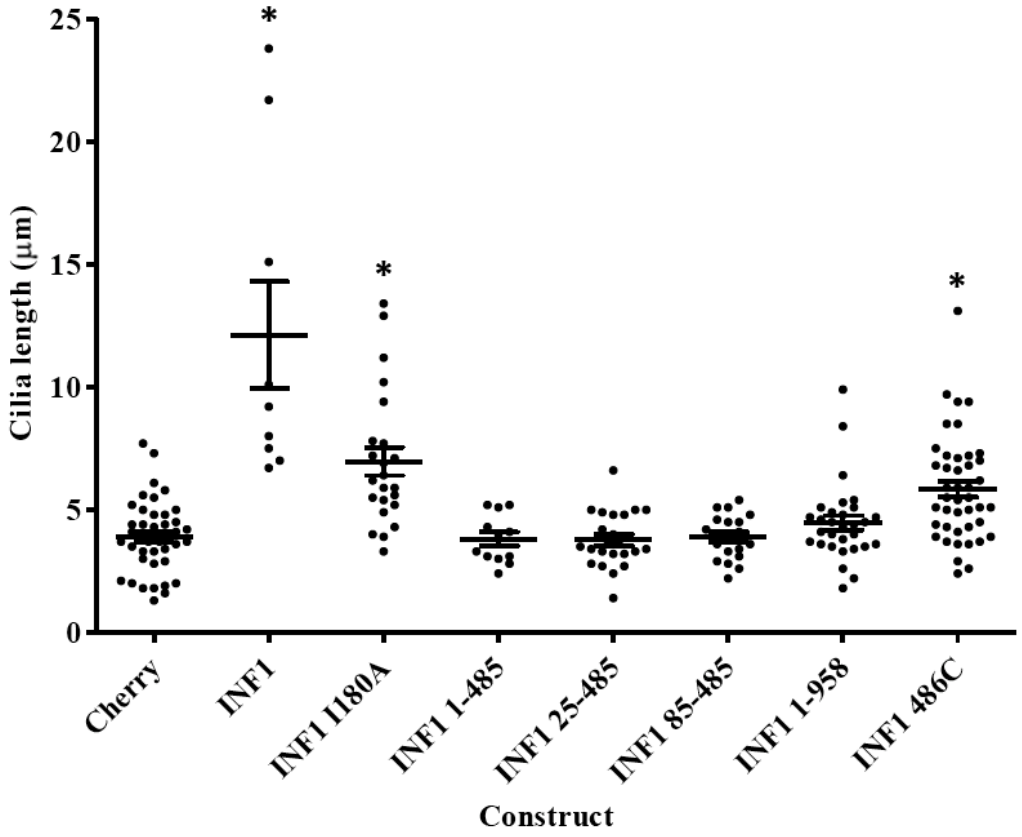

Figure 3.5.3. INF1 overexpression induces the formation of elongated cilia. INF1 full length and truncation derivatives were expressed in NIH-3T3 cells. Primary cilia were detected by an anti-acetylated tubulin antibody. Cilia lengths were measured using Northern Eclipse software. Cilia length was measured of cells that were counted in cilia presence assay (Figure 3.5.2). Data is presented as mean cilia length of one experiment +/- SD. * represents significant difference compared to Cherry control plasmid.

Chapter 4: Results Part II

4.1 Formin-Induced Coalignment of Actin and Microtubules, and Acetylation

Expression of constitutively active derivatives of the formin mDia1 induces cell elongation and coalignment of microtubules and actin stress fibers (Ishizaki et al., 2001). This effect is especially notable in "Kyoto" HeLa cells, a sub-clone of HeLa cells that normally exhibit a stereoptypical cuboidal morphology (Ishizaki et al., 2001). Given the previous observations with mDia1 and the effects of INF1 on actin and microtubule organization, I wanted to determine whether or not this effect is a general property of all formins. FH1+FH2 deletion derivatives of 13 of the 15 mammalian formins were expressed and their ability to induce actin and MT co-alignment in "Kyoto" HeLa cells was assessed. Results showed that expression of the FH1+FH2 containing derivatives of INF1, INF2, mDia1, mDia2, hDia2c, FMNL1, FMNL2, FMNL3, DAAM1, DAAM2, and mouse FMN1 formins were sufficient to induce end-to-end stress fiber formation and their co-alignment with microtubules in serum-starved Kyoto HeLa cells (Figure 4.1.1). Expression of equivalent FHOD1 and FHOD3 derivatives, however, did not induce stress fiber formation or actin-microtubule co-alignment. However, expression of longer derivatives of these proteins, FHOD1ΔDAD and FHOD3ΔN, were able to induce stress fiber formation and MT co-alignment (Figure 4.1.2).

In addition, many of these derivatives were sufficient to induce microtubule acetylation in NIH-3T3 cells (Figure 4.1.3). Previous experiments showed that a FH1+FH2 derivative of INF1 was able to induce microtubule acetylation. Interestingly, this derivative does not possess the MTBD. We wanted to determine if the FH1+FH2 domains of other formins were sufficient to induce microtubule acetylation. Results

showed that expression of the FH1+FH2 containing derivatives of INF1, mDia1, mDia2, hDia2, FMNL1, FMNL2, DAAM1, and DAAM2 were sufficient to induce microtubule acetylation (Figure 4.1.3). Expression of INF2, FMNL3, FHOD1, FHOD3, and mFMN1 p152 did not induce microtubule acetylation. Aside from FHOD1 and FHOD3, all constructs expressed had the ability to induce both actin stress fiber formation and microtubule acetylation.

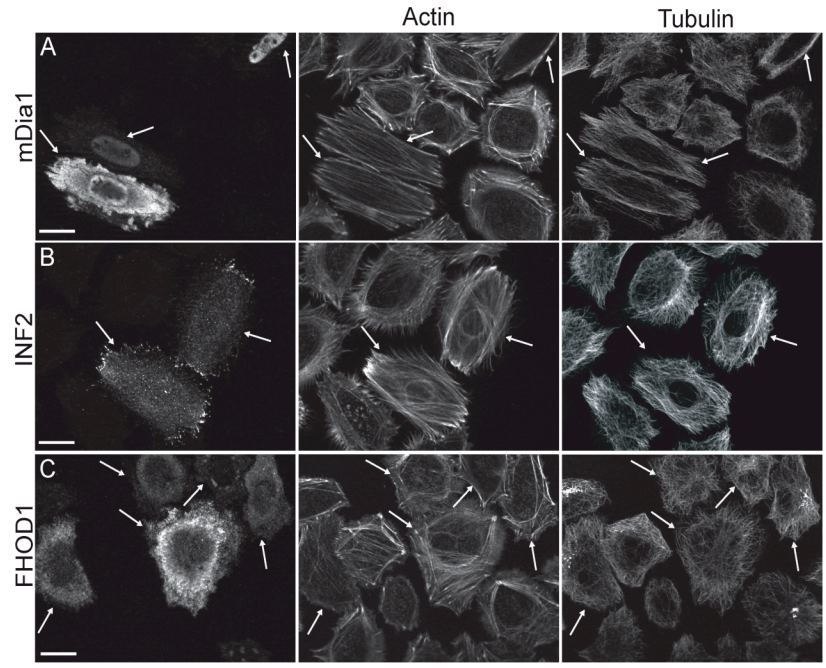

D

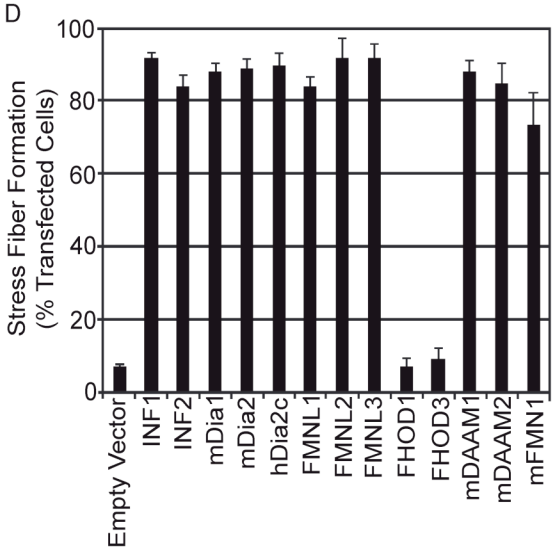

E

	Microtubule Alignment
Empty Vector	+
INF1	++++
INF2	++++
mDia1	++++
mDia2	+++
hDia2	+++
FMNL1	++++
FMNL2	+++
FMNL3	+++
FHOD1	+
FHOD3	+
mDAAM1	+++
mDAAM2	+++
mFMN1	+++

Figure 4.1.1. FH1+FH2 formin domains induce the formation of actin stress fibers and align microtubules. "Kyoto" HeLa cells were transfected with relevant constructs and grown in 10% FBS DMEM for 24hrs, then fixed in paraformaldehyde. (+) represents basal microtubule alignment, while (++++) indicates strong microtubule alignment. 0.5µg of each relevant construct was transfected. >50 cells were counted for each repeat. N=3.

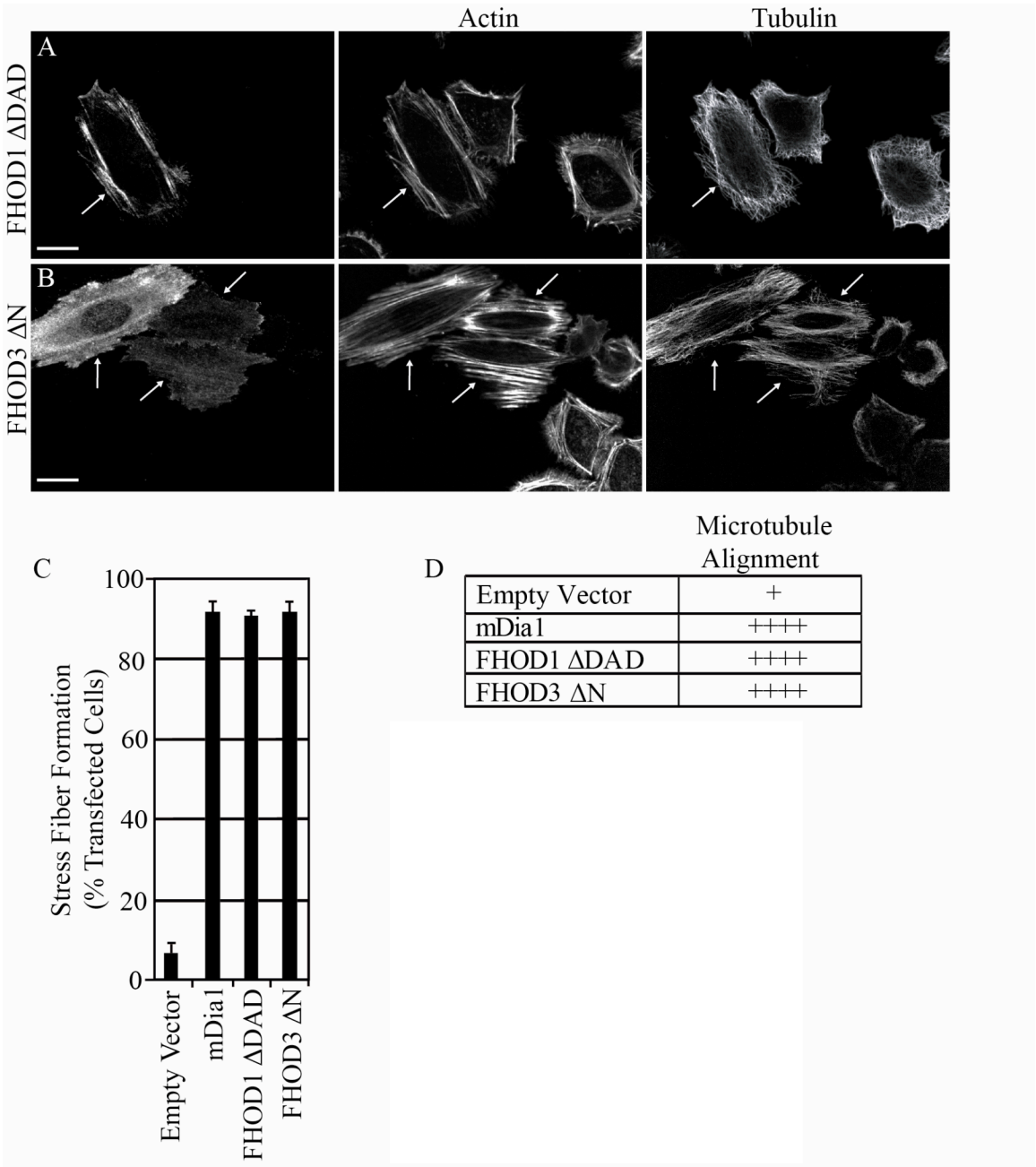

Figure 4.1.2. Longer versions of formins induce the formation of actin stress fibers and align microtubules. "Kyoto" HeLa cells were transfected with relevant constructs and grown in 10% FBS DMEM for 24hrs, then fixed in paraformaldehyde. (+) represents basal microtubule alignment, while (++++) indicates strong microtubule alignment. 0.5µg of relevant construct was transfected. >50 cells were counted for mDia1 and FHOD1ΔDAD, while <50 cells were counted for FHOD3ΔN. N=3. Data is shown as +SEM.

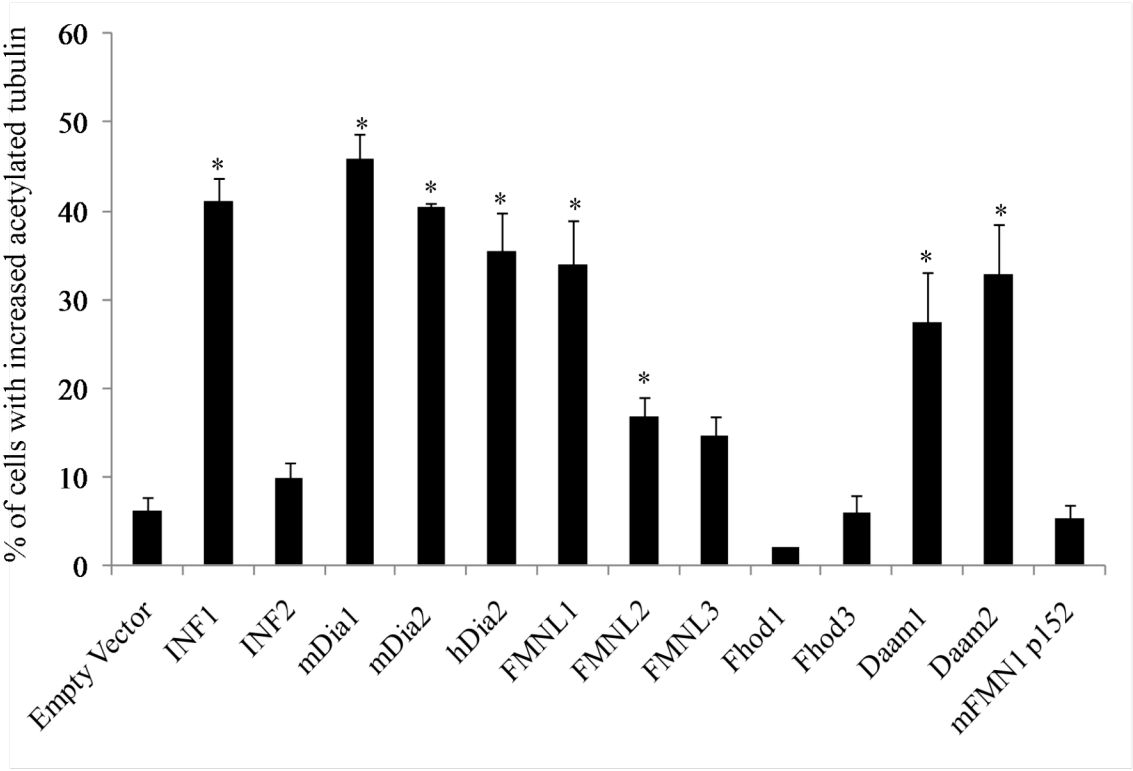

Figure 4.1.3. FH1+FH2 formin domains induce microtubule acetylation. NIH-3T3 cells were transfected with relevant constructs and grown in 0.5% DBS DMEM for 48hrs, then fixed in paraformaldehyde. 1µg of relevant construct was transfected. >50 cells were counted for each repeat. N=3. * indicates significance compared to empty vector control. Data was also contributed by S.Thurston.

Chapter 5: Discussion

5.1.1. Control of INF1-Induced Cytoskeletal Remodeling

The activity of most formins is controlled by internal autoregulatory domains. INF1, however, is constitutively active when over-expressed suggesting that it is not regulated through these means (Young et al., 2009; Higgs, 2005, and Figure 1.2). This observation prompted us to investigate other potential modes of regulation. In particular we addressed the role of MARK2 as a putative kinase regulator of INF1.

Microtubule-affinity regulating kinase 2 (MARK2) regulates the activity of other microtubule-associated proteins (MAPs) through phosphorylation at consensus K-X-G-S sites. Two of these sites can also be found in INF1 (Figure 3.1.7). Preliminary results from our laboratory showed that MARK2 was able to phosphorylate the INF1 C-terminus *in vitro* as well as inhibit INF1-induced microtubule acetylation. I wanted to confirm these results and determine if MARK2 is able to inhibit other aspects of INF1 activity.

INF1 has been shown to induce the polymerization of actin into thick stress fibers in NIH-3T3 cells (Young et al., 2008). Using immunofluorescence, we were able to show that co-expression of MARK2 inhibits INF1-induced actin stress fiber formation while expression of the kinase dead version had no obvious effect (Figures 3.1.1-3.1.3). Qualitatively, actin fibers were thinner and less abundant in cells that expressed both INF1 and MARK2, than in cells expressing INF1 and MARK2 kinase-dead or INF1 alone. Effects on stress fiber formation were not quantified because of the difficulty in differentiating between degrees of stress fiber formation. To obtain a more quantitative assessment of the effects of MARK2 expression on INF1 activity, an SRF reporter gene assay was used to measure changes in actin dynamics. In this assay, INF1-induced SRF

activation was also inhibited by MARK2 co-expression. In both assays, increasing the amount of transfected MARK2 plasmid increasingly inhibited INF1, suggesting INF1-induced actin stress fiber formation and actin polymerization may be inhibited by overcoming a high level of INF1 expression. After observing that MARK2 inhibits INF1-induced stress fiber formation, I wanted to identify the region of INF1 that was being targeted by MARK2.

MARK2 inhibited INF1's effects on actin dynamics and therefore it is likely inhibiting FH2 activity. To determine if the INF1 FH2 was targeted directly by MARK2, we overexpressed MARK2 with an INF1 plasmid corresponding to the first 485 amino acids of the protein (INF1 1-485), which encodes the INF1 FH1 and FH2 domains. In all readouts, we saw that this fragment was not inhibited by coexpression of MARK2, suggesting that the observed inhibitory effect of MARK2 on INF1 activity was likely being mediated by a motif in the INF1 C-terminus. INF1 contains many potential phosphorylation sites in its C-terminus. INF1 point mutants at serine-866 and serine-879 were made to determine if phosphorylation at the C-terminal K-X-G-S MARK2 consensus phosphorylation sites were responsible for INF1 inhibition by MARK2. All of the phosphomimetic (serine to aspartic acid) and unphosphorylatable (serine to alanine) INF1 point mutants maintained their ability to form actin stress fibers, associate with microtubules, acetylate microtubules, and disperse the Golgi. Counter to our expectations, however, the ability of the S879A mutant to activate the SRF pathway was significantly reduced. One explanation for this result is the potential misfolding of the INF1 S879A protein, rendering it inactive or targeted for degradation. Although the S879A result is inconsistent with results from the stress fiber formation assay, it may be

due to the qualitative nature of immunofluorescence results. These results suggest that INF1 is not regulated by phosphorylation at these sites. However, it is possible that INF1 may be inhibited by phosphorylation at other serine/threonine residues, or that individual serine mutations are insufficient to induce a measurable change in regulatory activity.

INF1 is a microtubule binding protein and INF1 expression induces microtubule acetylation and stabilization (Young et al., 2008). I tested the ability of MARK2 to inhibit INF1-induced microtubule acetylation and INF1 assocation with MTs. Despite preliminary findings by Kevin Young that suggested MARK2 inhibits INF1-induced MT acetylation, I found that MARK2 over-expression did not affect INF1-induced MT acetylation or MT binding by INF1. It is not clear why this should be the case, although one possibility lies in the INF1 derivatives used in these assays. The preliminary data was obtained using a C-terminally tagged INF1 derivative while my data was obtained using a protein with an N-terminal tag. The C-terminal YFP tag was later shown to interfere with INF1-induced Golgi dispersion. Therefore one explanation for the earlier observation may be that the C-terminal YFP tag inhibits MTBD-induced microtubule acetylation while MARK2 co-expression inhibits FH2-dependent effects on MT acetylation.

Our lab has shown that overexpression of INF1 induces the dispersion of the Golgi into mini-stacks (Sarah Copeland, personal communication). Dispersion of the Golgi by INF1 is dependent on the function of the INF1 MTBD and FH2 domain; mutations affecting either activity compromise the ability of INF1to induce fragmentation of the Golgi (Sarah Copeland, unpublished results). Given that the effect of INF1 on Golgi is FH2-dependent, it was anticipated that MARK2 would inhibit INF1-induced Golgi dispersion. I found, however, that overexpression of MARK2 did not affect INF1-

induced Golgi dispersion. Two alternative hypotheses can be considered to explain this observation. One is that the effects of INF1 on the Golgi are not dependent on effects on actin dynamics. However, this is unlikely since an INF1 I180A mutant, which does not affect actin, also does not disperse the Golgi. The other is that the inhibition of INF1 by MARK2 is not complete (as seen in the SRF assay) and perhaps the remaining activity of INF1 is sufficient to induce Golgi dispersion.

5.1.2. Regulation of Formins by Par1b

Par1b has been shown to form a complex with, and regulate the function of GEF-H1, an activator of RhoA. This finding is important because RhoA induces the formation of actin stress fibers, through alleviating autoinhibition of diaphanous-related formins. Through phosphorylation of serine residues 885 and 959, Par1b inactivates GEF-H1's nucleotide exchange activity, thereby inhibiting activation of RhoA (Yamahashi et al., 2011). Interestingly, phosphorylation of GEF-H1 took place at R-X-X-S and R-X-X-X-S sites and not at K-X-G-S sequences, which have previously been shown to be MARK2 consensus phosphorylation sites (Yamahasi et al., 2011). This is significant because INF1 possesses many R-X-X-S and R-X-X-X-S sites, with many being in its microtubule binding domain region.

Interestingly, Par1b has also been shown to inhibit GEF-H1-induced microtubule acetylation and microtubule binding (Ren et al., 1998, Yoshimura and Miki, 2011). Par1b binds and phosphorylates GEF-H1 at serine residues, inducing microtubule depolymerization and alleviating GEF-H1-microtubule interactions, by potentially inhibiting GEF-H1's guanine nucleotide exchange factor activity on Rho.

5.1.3. Par1b and Polarity in Epithelial Cells and Fibroblasts

Aside from its effects on actin polymerization, we have shown that Par-1b/MARK2 does not play a role in regulating INF1-induced cell polarity of NIH-3T3 fibroblasts. Conversely, a role of Par-1b in other cell types has been reported. As previously mentioned, Par1b seems to be involved in mammalian epithelial cell polarity, specifically in the formation of tight junctions. However, observations regarding Par1b's involvement in cell polarity seem to be restricted to mammalian epithelial cells, *Drosophila* oocytes during oogenesis, and *C.elegans* during anterior-posterior establishment (Suzuki et al., 2004, Guo and Kemphues, 1995). Therefore, it may be interesting to coexpress MARK2 with INF1 in epithelial cells to determine if MARK2 inhibition of INF1-induced microtubule acetylation and Golgi dispersion is cell-type dependent.

5.2.1. INF1 Inhibits Cilia Formation

Primary cilia are highly enriched for acetylated tubulin and are easy to detect with an acetylated tubulin antibody as a short cable extending from the perinuclear region. While investigating INF1-induced MT acetylation it was noted that INF1-expressing cells failed to form a primary cilium. Overexpression of INF1 I180A, which does not disperse the Golgi or induce F-actin accumulation, did not inhibit cilia formation to the same extent as wild-type INF1-expressing cells. Similarly, expression of INF1 1-958, which induces F-actin formation, but does not disperse the Golgi, failed to inhibit cilia formation. These observations suggest a link between INF1-induced Golgi dispersion and inhibition of cilia formation.

Cilia formation in fibroblasts is characterized by a primary ciliary vesicle, derived from the Golgi body, forming a sheath around the mother centriole. The primary cilium grows by extension within the sheath, which itself grows through fusion of secondary vesicles from the Golgi (Sorokin, 1968; Ghossoub et al., 2011). Although our lab has shown that protein trafficking remains intact upon Golgi dispersal, formation of primary and secondary ciliary sheath vesicles may be disrupted.

Although not present in most INF1-expressing cells, when cilia were present, they were much longer than in control cells. However, results obtained from overexpressing additional INF1 derivatives indicates that this effect is independent of INF1's ability to polymerize F-actin, disperse the Golgi, and stabilize microtubules. Rather, it suggests that INF1 uses a separate mechanism to stimulate cilia growth. Meanwhile, expression of INF1 I180A and INF1 486C induced the formation of intermediate length cilia. The formation of intermediate length cilia by overexpressing the INF1 486C fragment, suggests a role for the C-terminus in stimulating cilia growth. This idea is supported by the formation of normal length cilia by cells expressing INF1 fragments that do not possess the C-terminus.

5.3.1. Formin FH1-FH2 Derivatives Induce Actin and Microtubule Alignment, as well as Microtubule Acetylation

Expression of the FH1-FH2 domains of mDia1 has been shown to be sufficient to induce F-actin stress fiber formation, cell elongation and microtubule alignment with actin filaments in HeLa cells (Ishizaki et al., 2001). We confirmed the effect of mDia1 FH1-FH2 expression and showed that FH1-FH2 derivatives of nearly all mammalian formins induce the same characteristic cell morphology with the exception of FHOD1

and FHOD3 (Figure 4.1.1). In addition, we show that many of the FH1-FH2 derivatives are also able to induce microtubule acetylation in NIH-3T3 cells. Derivatives fell into three categories of acetylation activity: acetylators, moderate acetylators, and non-acetylators. INF1, mDia1, mDia2, hDia2, FMNL1, DAAM1, and DAAM2 were acetylators; INF2, FMNL2, and FMNL3 were shown to be moderate acetylators; and FHOD1, FHOD3, and mFMN1 were non-acetylators. Aside from INF2 and FMNL3, the derivatives that are able to induce F-actin formation, cell elongation, and microtubule alignment, also induce microtubule acetylation. Meanwhile, FHOD1 and FHOD3 derivatives, which were unable to induce stress fibers or align microtubules with actin, also failed to induce microtubule acetylation. This suggests a potential link between the ability to regulate the actin cytoskeleton and microtubule stability.

In contrast to the FH1-FH2 derivatives, longer versions of FHOD1 and FHOD3, FHOD1ΔDAD and FHOD3ΔN, are also able to induce F-actin formation, cell elongation, and microtubule alignment when expressed in Hela cells (Figure 4.1.2). We were unable to express the FHOD1ΔDAD construct in NIH-3T3 cells, however, FHOD3ΔN was able to induce microtubule acetylation and SRF activation in these cells (Susan Thurston and John Copeland, unpublished results), These results indicate that the FH1-FH2 of FHOD3 are not sufficient, but most likely necessary to induce both actin and microtubule modifications.

5.3.2. Conclusion

INF1 is a constitutively active formin and does not contain any of the previously described formin autoinhibitory regulatory domains. We have shown that MARK2 co-expression inhibits INF1-induced stress fiber formation and INF1-induced activation the MAL/SRF transcription pathway. Our analysis shows that this inhibition of FH2 activity is occurring at INF1's C-terminus. However, MARK2 is unable to inhibit the association of INF1 with microtubules, INF1-induced microtubule acetylation and INF1-induced Golgi dispersion.

In addition to its known functions, INF1 overexpression inhibits the formation of primary cilia. Using INF1 truncation derivatives, INF1's ability to disrupt cilia formation was shown to correlate with INF1's ability to disperse the Golgi. In rare instances, however, INF1 overexpression causes the formation of cilia of abnormally long length. This effect on cilia length is associated with the INF1 MTBD and seems to be modified by FH2 activity as the presence of both functional motifs has synergistic effect on cilia growth.

These findings suggest a novel mode of INF1 regulation and contribute to our understanding of INF1's role as a key player in both the actin and microtubule cytoskeleton networks.

References

Abdul-Majeed, S., Moloney, B.C. & Nauli, S.M., 2011. Mechanisms regulating cilia growth and cilia function in endothelial cells. Cellular and Molecular Life Sciences: CMLS.

Abd-El-Bar, M.M., et al., 2007. Impaired photoreceptor protein transport and synaptic transmission in a mouse model of Bardet-Biedl syndrome. Vision Research, 47, pp.1019-1024.

Ackmann, M., Wiech, H. & Mandelkow, Eckhard, 2000. Nonsaturable Binding Indicates Clustering of Tau on the Microtubule Surface in a Paired Helical Filament-like Conformation. Journal of Biological Chemistry, 275(39), pp.30335 -30343.

Akella, J.S. et al., 2010. MEC-17 is an [agr]-tubulin acetyltransferase. Nature, 467(7312), pp.218-222.

Alberts, A.S., 2001. Identification of a Carboxyl-terminal Diaphanous-related Formin Homology Protein Autoregulatory Domain. Journal of Biological Chemistry, 276(4), pp.2824 -2830.

Astin, J.W. et al., 2010. Competition amongst Eph receptors regulates contact inhibition of locomotion and invasiveness in prostate cancer cells. Nat Cell Biol, 12(12), pp.1194-1204.

Augustinack, J. et al., 2002. Specific tau phosphorylation sites correlate with severity of neuronal cytopathology in Alzheimer's disease. Acta Neuropathologica, 103, pp.26-35.

Azimzadeh, J. & Marshall, W.F., 2010. Building the centriole. Current Biology: CB, 20(18), pp.R816-825.

Bartolini, F. et al., 2008. The formin mDia2 stabilizes microtubules independently of its actin nucleation activity. The Journal of Cell Biology, 181(3), pp.523-536.

Bentley, D. & Toroian-Raymond, A., 1986. Disoriented pathfinding by pioneer neurone growth cones deprived of filopodia by cytochalasin treatment. Nature, 323(6090), pp.712-715.

Berbari, N.F. et al., 2009. The Primary Cilium as a Complex Signaling Center. Current Biology, 19(13), p.R526-R535.

Bos, J.L., Rehmann, H. & Wittinghofer, A., 2007. GEFs and GAPs: critical elements in the control of small G proteins. Cell, 129(5), pp.865-877.

Brazelton, W.J. et al., 2001. The bld1 mutation identifies the Chlamydomonas osm-6 homolog as a gene required for flagellar assembly. Current Biology, 11(20), pp.1591-1594.

Cash, A.D. et al., 2003. Microtubule reduction in Alzheimer's Disease and aging is independent of tau filament formation. American Journal of Pathology, 162, pp. 1623-1627.

Chabin-Brion, K. et al., 2001. The Golgi Complex Is a Microtubule-organizing Organelle. Molecular Biology of the Cell, 12(7), pp.2047 -2060.

Chen, Y.M. et al., 2006. Microtubule affinity-regulating kinase 2 functions downstream of the PAR-3/PAR-6/atypical PKC complex in regulating hippocampal neuronal polarity. Proceedings of the National Academy of Sciences, 103(22), pp.8534 -8539.

Chhabra, E.S. & Higgs, H.N., 2007. The many faces of actin: matching assembly factors with cellular structures. Nature Cell Biology, 9(10), pp.1110-1121.

Cohen, T.J. et al., 2011. The acetylation of tau inhibits its function and promotes pathological tau aggregation. Nat Commun, 2, p.252.

Cramer, L.P., Siebert, M. & Mitchison, T.J., 1997. Identification of Novel Graded Polarity Actin Filament Bundles in Locomoting Heart Fibroblasts: Implications for the Generation of Motile Force. The Journal of Cell Biology, 136(6), pp.1287 -1305.

Cripps, D. et al., 2006. Alzheimer Disease-specific Conformation of Hyperphosphorylated Paired Helical Filament-Tau Is Polyubiquitinated through Lys-48, Lys-11, and Lys-6 Ubiquitin Conjugation. Journal of Biological Chemistry, 281(16), pp.10825 -10838.

Daub, H. et al., 2001. Rac/Cdc42 and p65PAK regulate the microtubule-destabilizing protein stathmin through phosphorylation at serine 16. The Journal of Biological Chemistry, 276(3), pp.1677-1680.

Dorval, V. & Fraser, P.E., 2006. Small Ubiquitin-like Modifier (SUMO) Modification of Natively Unfolded Proteins Tau and α-Synuclein. Journal of Biological Chemistry, 281(15), pp.9919 -9924.

Dossou, S.J.Y., Bré, M. & Hallworth, R., 2007. Mammalian cilia function is independent of the polymeric state of tubulin glycylation. Cell Motility and the Cytoskeleton, 64(11), pp.847-855.

Drewes, Gerard, Ebneth, A. & Mandelkow, Eva-Maria, 1998. MAPs, MARKs and microtubule dynamics. Trends in Biochemical Sciences, 23(8), pp.307-311.

Dryden, S.C. et al., 2003. Role for human SIRT2 NAD-dependent deacetylase activity in control of mitotic exit in the cell cycle. Molecular and Cellular Biology, 23(9), pp.3173-3185.

Dunn, S. et al., 2008. Differential trafficking of Kif5c on tyrosinated and detyrosinated microtubules in live cells. Journal of Cell Science, 121(7), pp.1085 -1095.

Ebneth, A. et al., 1999. Phosphorylation of MAP2c and MAP4 by MARK kinases leads to the destabilization of microtubules in cells. Cytoskeleton, 44(3), pp. 209-224.

Efimov, A. et al., 2007. Asymmetric CLASP-dependent nucleation of noncentrosomal microtubules at the trans-Golgi network. Developmental Cell, 12(6), pp.917-930.

Etienne-Manneville, Sandrine & Hall, Alan, 2003. Cdc42 regulates GSK-3[beta] and adenomatous polyposis coli to control cell polarity. Nature, 421(6924), pp.753-756.

Fukata, M. et al., 2002. Rac1 and Cdc42 Capture Microtubules through IQGAP1 and CLIP-170. Cell, 109(7), pp.873-885.

Galjart, N., 2005. CLIPs and CLASPs and cellular dynamics. Nat Rev Mol Cell Biol, 6(6), pp.487-498.

Gasteier, J.E. et al., 2003. Activation of the Rac-binding Partner FHOD1 Induces Actin Stress Fibers via a ROCK-dependent Mechanism. Journal of Biological Chemistry, 278(40), pp.38902 -38912.

Geneste, O., Copeland, JW. & Treisman, R. LIM kinase and Diaphanous cooperate to regulate serum response factor and actin dynamics. J Cell Bio, 157 (5), pp.831-838.

Ghossoub, R. et al., 2011. The ciliary pocket: a once-forgotten membrane domain at the base of cilia. Biology of the Cell, 103(3), pp.131-144.

Goetz, S.C. & Anderson, K.V., 2010. The primary cilium: a signalling centre during vertebrate development. Nature Reviews. Genetics, 11(5), pp.331-344.

Goley, E.D. & Welch, M.D., 2006. The ARP2/3 complex: an actin nucleator comes of age. Nat Rev Mol Cell Biol, 7(10), pp.713-726.

Gomes, E.R., Jani, S. & Gundersen, G.G., 2005. Nuclear movement regulated by Cdc42, MRCK, myosin, and actin flow establishes MTOC polarization in migrating cells. Cell, 121(3), pp.451-463.

Gomez, T.S. et al., 2007. Formins regulate the Arp2/3-independent polarization of the MTOC to the Immunological Synapse. Immunity, 26(2), pp.177-190.

Govek, E.-E., Hatten, M.E. & Van Aelst, L., 2011. The role of Rho GTPase proteins in CNS neuronal migration. Developmental Neurobiology, 71(6), pp.528-553.

Grundke-Iqbal, I. et al., 1986. Microtubule-associated protein tau. A component of Alzheimer paired helical filaments. Journal of Biological Chemistry, 261(13), pp.6084 -6089.

Guo, S. & Kemphues, K.J., 1995. par-1, a gene required for establishing polarity in C. elegans embryos, encodes a putative Ser/Thr kinase that is asymmetrically distributed. Cell, 81(4), pp.611-620.

Hammond, J., Cai, D. & Verhey, Kristen J., 2008. Tubulin modifications and their cellular functions. Current Opinion in Cell Biology, 20(1), pp.71-76.

Harris, K.P. & Tepass, U., 2010. Cdc42 and vesicle trafficking in polarized cells. Traffic (Copenhagen, Denmark), 11(10), pp.1272-1279.

Haycraft, C.J. et al., 2005. Gli2 and gli3 localize to cilia and require the intraflagellar transport protein polaris for processing and function. PLoS Genetics, 1, pp. e53.

Higgs, H.N., 2005. Formin proteins: a domain-based approach. Trends in Biochemical Sciences, 30(6), pp.342-353.

Higgs, H.N. & Peterson, K.J., 2005. Phylogenetic analysis of the formin homology 2 domain. Molecular Biology of the Cell, 16(1), pp.1-13.

Hildebrandt, F., Benzing, T. & Katsanis, N., 2011. Ciliopathies. The New England Journal of Medicine, 364(16), pp.1533-1543.

Hotulainen, P. & Lappalainen, P., 2006. Stress fibers are generated by two distinct actin assembly mechanisms in motile cells. The Journal of Cell Biology, 173, pp. 383-394.

Hou, Y. et al., 2007. Functional analysis of an individual IFT protein: IFT46 is required for transport of outer dynein arms into flagella. The Journal of Cell Biology, 176(5), pp.653 -665.

Huang, J.D. et al., 1999. Direct interaction of microtubule- and actin-based transport motors. Nature, 397(6716), pp.267-270.

Hubbert, C. et al., 2002. HDAC6 is a microtubule-associated deacetylase. Nature, 417(6887), pp.455-458.

Hurov, J. & Piwnica-Worms, Helen, 2007. The Par-1/MARK family of protein kinases: from polarity to metabolism. Cell Cycle (Georgetown, Tex.), 6(16), pp.1966-1969.

Hwang, E. et al., 2003. Spindle orientation in Saccharomyces cerevisiae depends on the transport of microtubule ends along polarized actin cables. The Journal of Cell Biology, 161(3), pp.483-488.

Iomini, C. et al., 2009. Retrograde Intraflagellar Transport Mutants Identify Complex A Proteins With Multiple Genetic Interactions in Chlamydomonas reinhardtii. Genetics, 183(3), pp.885 -896.

Ishikawa, H. & Marshall, W.F., 2011. Ciliogenesis: building the cell's antenna. Nat Rev Mol Cell Biol, 12(4), pp.222-234.

Ishizaki, T. et al., 2001. Coordination of microtubules and the actin cytoskeleton by the Rho effector mDia1. Nature Cell Biology, 3(1), pp.8-14.

Kemphues, K., 2000. PARsing embryonic polarity. Cell, 101(4), pp.345-348.

Kevin T., V., 2005. Microtubule plus ends, motors, and traffic of Golgi membranes. Biochimica et Biophysica Acta (BBA) - Molecular Cell Research, 1744(3), pp.316-324.

King, M.E. et al., 2006. Tau-dependent microtubule disassembly initiated by prefibrillar β-amyloid. The Journal of Cell Biology, 175(4), pp.541 -546.

Kodama, A. et al., 2003. ACF7: An essential integrator of microtubule dynamics. Cell, 115(3), pp.343-354.

Kodani, A. & Sütterlin, Christine, 2008. The Golgi protein GM130 regulates centrosome morphology and function. Molecular Biology of the Cell, 19(2), pp.745-753.

Kovar, D. et al., 2006. Control of the assembly of ATP- and ADP-actin by formins and profilin. Cell, 124, pp. 423-435.

Kollman, J.M. et al., 2011. Microtubule nucleation by γ-tubulin complexes. Nat Rev Mol Cell Biol, 12(11), pp.709-721.

Kroschewski, R., Hall, A & Mellman, I, 1999. Cdc42 controls secretory and endocytic transport to the basolateral plasma membrane of MDCK cells. Nature Cell Biology, 1(1), pp.8-13.

Kulaga, H.M. et al., 2004. Loss of BBS proteins causes anosmia in humans and defects in olfactory cilia structure and function in the mouse. Nature Genetics, 36, pp.994-998.

Kupfer, A., Dennert, G. & Singer, S.J., 1983. Polarization of the Golgi apparatus and the microtubule-organizing center within cloned natural killer cells bound to their targets. Proceedings of the National Academy of Sciences of the United States of America, 80(23), pp.7224-7228.

Lafanechere, L. et al., 1998. Suppression of tubulin tyrosine ligase during tumor growth. Journal of Cell Science, 111(2), pp.171 -181.

Lazarides, E. & Burridge, K, 1975. Alpha-actinin: immunofluorescent localization of a muscle structural protein in nonmuscle cells. Cell, 6(3), pp.289-298.

Ledesma, M.D. et al., 1994. Analysis of microtubule-associated protein tau glycation in paired helical filaments. The Journal of Biological Chemistry, 269(34), pp.21614-21619.

Lee, J.S.H. et al., 2005. Cdc42 Mediates Nucleus Movement and MTOC Polarization in Swiss 3T3 Fibroblasts under Mechanical Shear Stress. Molecular Biology of the Cell, 16(2), pp.871-880.

Leung, T. et al., 1996. The p160 RhoA-binding kinase ROK alpha is a member of a kinase family and is involved in the reorganization of the cytoskeleton. Molecular and Cellular Biology, 16(10), pp.5313-5327.

Levitan, D.J. et al., 1994. par-2, a gene required for blastomere asymmetry in Caenorhabditis elegans, encodes zinc-finger and ATP-binding motifs. Proceedings of the National Academy of Sciences of the United States of America, 91(13), pp.6108-6112.

Li, F. & Higgs, H.N., 2005. Dissecting requirements for auto-inhibition of actin nucleation by the formin, mDia1. Journal of Biological Chemistry, 280, pp 6986-6992.

Li, Y. & Hu, J., 2011. Small GTPases and cilia. Protein & Cell, 2(1), pp.13-25.

Lim, Y.S., Chua, C.E.L. & Tang, B.L., 2011. Rabs and other small GTPases in ciliary transport. Biology of the Cell / Under the Auspices of the European Cell Biology Organization, 103(5), pp.209-221.

Lowe, M., 2011. Structural organization of the Golgi apparatus. Current Opinion in Cell Biology, 23(1), pp.85-93.

Lu, H. et al., 2009. Role of Partitioning-defective 1/Microtubule Affinity-regulating Kinases in the Morphogenetic Activity of Helicobacter pylori CagA. Journal of Biological Chemistry, 284(34), pp.23024 -23036.

Luders, J. & Stearns, T., 2007. Microtubule-organizing centres: a re-evaluation. Nat Rev Mol Cell Biol, 8(2), pp.161-167.

Maekawa, M. et al., 1999. Signaling from Rho to the actin cytoskeleton through protein kinases ROCK and LIM-kinase. Science (New York, N.Y.), 285(5429), pp.895-898.

Magdalena, J. et al., 2003. Involvement of the Arp2/3 complex and Scar2 in Golgi polarity in scratch wound models. Molecular Biology of the Cell, 14(2), pp.670-684.

Mandato, C.A. & Bement, W.M., 2003. Actomyosin transports microtubules and microtubules control actomyosin recruitment during Xenopus oocyte wound healing. Current Biology: CB, 13(13), pp.1096-1105.

Martin, L., 2011. Structural organization of the Golgi apparatus. Current Opinion in Cell Biology, 23(1), pp.85-93.

Marx, A. et al., 2006. Interaction of kinesin motors, microtubules, and MAPs. Journal of Muscle Research and Cell Motility, 27(2), pp.125-137.

Matenia, D. & Mandelkow, Eva-Maria, 2009. The tau of MARK: a polarized view of the cytoskeleton. Trends in Biochemical Sciences, 34(7), pp.332-342.

Mironov, A.A. & Beznoussenko, G.V., 2011. Molecular mechanisms responsible for formation of Golgi ribbon. Histology and Histopathology, 26(1), pp.117-133.

Mishima, M. et al., 2007. Structural basis for tubulin recognition by cytoplasmic linker protein 170 and its autoinhibition. Proceedings of the National Academy of Sciences of the United States of America, 104(25), pp.10346-10351.

Miyasaka, T. et al., 2005. Visualization of newly deposited tau in neurofibrillary tangles and neuropil threads. Journal of Neuropathology and Experimental Neurology, 64(8), pp.665-674.

Miyoshi, K. et al., 2011. Factors that influence primary cilium length. Acta Medica Okayama, 65(5), pp.279-285.

Moseley, J.B. et al., 2004. A conserved mechanism for Bni1- and mDia1-induced actin assembly and dual regulation of Bni1 by Bud6 and profilin. Molecular Biology of the Cell, 15(2), pp.896-907.

Naumanen, P., Lappalainen, P. & Hotulainen, P., 2008. Mechanisms of actin stress fibre assembly. Journal of Microscopy, 231(3), pp.446-454.

Nelson, J.W. 2000. W(H)ither the Golgi during mitosis? Journal of Cell Biology, 149(2), pp. 243-248.

Nur Firat-Karalar, E., & Welch M, M.W., 2010. New mechanisms and functions of actin nucleation. Current Opinion in Cell Biology, 23(1), pp. 4-13.

Ora, B., 2007. Lim kinases, regulators of actin dynamics. The International Journal of Biochemistry & Cell Biology, 39(6), pp.1071-1076.

Ozer, R.S. & Halpain, S., 2000. Phosphorylation-dependent Localization of Microtubule-associated Protein MAP2c to the Actin Cytoskeleton. Molecular Biology of the Cell, 11(10), pp.3573-3587.

Palazzo, A.F. et al., 2001. mDia mediates Rho-regulated formation and orientation of stable microtubules. Nat Cell Biol, 3(8), pp.723-729.

Park, A.S. & Pollard, T.D., 2009. Review of the mechanism of processive actin filament elongation by formins. Cell Motil Cytoskeleton, 66(8), pp. 606-617.

Pazour, G.J. & Witman, G.B., 2003. The vertebrate primary cilium is a sensory organelle. Current Opinion in Cell Biology, 15(1), pp.105-110.

Pazour, G.J. et al., 2000. Chlamydomonas IFT88 and Its Mouse Homologue, Polycystic Kidney Disease Gene Tg737, Are Required for Assembly of Cilia and Flagella. The Journal of Cell Biology, 151(3), pp.709 -718.

Pazour, G.J. et al., 2002. Polycystin-2 localizes to kidney cilia and the ciliary level is elevated in orpk mice with polycystic kidney disease. Current Biology: CB, 12(11), pp.R378-380.

Pedersen, L.B. et al., 2008. Assembly of primary cilia. Developmental Dynamics, 237(8), pp.1993-2006.

Pellegrin, S. & Mellor, H., 2007. Actin stress fibers. Journal of Cell Science, 120(20), pp.3491 -3499.

Peng, J. et al., 2003. Disruption of the Diaphanous-Related Formin Drf1 Gene Encoding mDia1 Reveals a Role for Drf3 as an Effector for Cdc42. Current Biology, 13(7), pp.534-545.

Perdiz, D. et al., 2011. The ins and outs of tubulin acetylation: more than just a post-translational modification? Cellular Signalling, 23(5), pp.763-771.

Piperno, G. et al., 1998. Distinct Mutants of Retrograde Intraflagellar Transport (IFT) Share Similar Morphological and Molecular Defects. The Journal of Cell Biology, 143(6), pp.1591 -1601.

Poole, C.A., Zhang, Z.-J. & Ross, J.M., 2001. The differential distribution of acetylated and detyrosinated alpha-tubulin in the microtubular cytoskeleton and primary cilia of hyaline cartilage chondrocytes. Journal of Anatomy, 199(Pt 4), pp.393-405.

Pritchard, C.A. et al., 2004. B-Raf Acts via the ROCKII/LIMK/Cofilin Pathway To Maintain Actin Stress Fibers in Fibroblasts. Molecular and Cellular Biology, 24(13), pp.5937 -5952.

Pugacheva, E.N. et al., 2007. HEF1-dependent Aurora A activation induces disassembly of the primary cilium. Cell, 129(7), pp.1351-1363.

Qiang, L. et al., 2006. Tau Protects Microtubules in the Axon from Severing by Katanin. The Journal of Neuroscience, 26(12), pp.3120 -3129.

Redeker, V. et al., 2005. Mutations of tubulin glycylation sites reveal cross-talk between the C termini of alpha- and beta-tubulin and affect the ciliary matrix in Tetrahymena. The Journal of Biological Chemistry, 280(1), pp.596-606.

Reed, N.A. et al., 2006. Microtubule Acetylation Promotes Kinesin-1 Binding and Transport. Current Biology, 16(21), pp.2166-2172.

Ren, Y. et al., 1998. Cloning and characterization of GEF-H1, a microtubule-associated guanine nucleotide exchange factor for Rac and Rho GTPases. The Journal of Biological Chemistry, 273(52), pp.34954-34960.

Ridley, A J & Hall, A, 1992. The small GTP-binding protein rho regulates the assembly of focal adhesions and actin stress fibers in response to growth factors. Cell, 70(3), pp.389-399.

Ridley, A J et al., 1992. The small GTP-binding protein rac regulates growth factor-induced membrane ruffling. Cell, 70(3), pp.401-410.

Ridley, Anne J., 2011. Life at the Leading Edge. Cell, 145(7), pp.1012-1022.

Ridley, Anne J. et al., 2003. Cell Migration: Integrating Signals from Front to Back. Science, 302(5651), pp.1704 -1709.

Rivero, S., et al., 2009. Microtubule nucleation at the cis-side of the Golgi apparatus requires AKAP450 and GM130. The EMBO Journal, 28, pp. 1016-1028.

Rodman, J.S. & Wandinger-Ness, A., 2000. Rab GTPases coordinate endocytosis. Journal of Cell Science, 113(2), pp.183-192.

Roll-Mecak, A. & McNally, F.J., 2010. Microtubule-severing enzymes. Current Opinion in Cell Biology, 22(1), pp.96-103.

Rosenbaum, J.L. & Witman, G.B., 2002. Intraflagellar transport. Nature Reviews. Molecular Cell Biology, 3(11), pp.813-825.

Rydholm, S., et al., 2010. Mechanical properties of primary cilia regulate the response to fluid flow. American Journal of Physiology – Renal Physiology, 298, pp. 1096-1102.

Scholey, J.M., 2003. Intraflagellar transport. Annual Review of Cell and Developmental Biology, 19, pp.423-443.

Schönichen, A. & Geyer, M., 2010. Fifteen formins for an actin filament: A molecular view on the regulation of human formins. Biochimica et Biophysica Acta (BBA) - Molecular Cell Research, 1803(2), pp.152-163.

Seeley, E.S. & Nachury, M.V., 2010. The perennial organelle: assembly and disassembly of the primary cilium. Journal of Cell Science, 123(Pt 4), pp.511-518.

Sfakianos, J. et al., 2007. Par3 Functions in the Biogenesis of the Primary Cilium in Polarized Epithelial Cells. The Journal of Cell Biology, 179(6), pp.1133-1140.

Shida, T. et al., 2010. The major α-tubulin K40 acetyltransferase αTAT1 promotes rapid ciliogenesis and efficient mechanosensation. Proceedings of the National Academy of Sciences of the United States of America, 107(50), pp.21517-21522.

Small, J V, 1988. The actin cytoskeleton. Electron Microscopy Reviews, 1(1), pp.155-174.

Small, J.V. et al., 2002. The lamellipodium: where motility begins. Trends in Cell Biology, 12, pp.112-120.

Sorokin, S.P., 1968. Reconstructions of Centriole Formation and Ciliogenesis in Mammalian Lungs. Journal of Cell Science, 3(2), pp.207 -230.

Sotiropoulos, A. et al., 1999. Signal-regulated activation of serum response factor is mediated by changes in actin dynamics. Cell, 98(2), pp. 159-169.

Sütterlin, C. et al., 2002. Fragmentation and dispersal of the pericentriolar Golgi complex is required for entry into mitosis in mammalian cells. Cell, 109(3), pp.359-369.

Sütterlin, C & Colanzi, A., 2010. The Golgi and the centrosome: building a functional partnership. The Journal of Cell Biology, 188(5), pp.621-628.

Sütterlin, C. et al., 2001. Polo-like kinase is required for the fragmentation of pericentriolar Golgi stacks during mitosis. Proceedings of the National Academy of Sciences, 98(16), pp.9128 -9132.

Sütterlin, C. et al., 2005. The Golgi-associated protein GRASP65 regulates spindle dynamics and is essential for cell division. Molecular Biology of the Cell, 16(7), pp.3211-3222.

Suzuki, A. et al., 2004. aPKC acts upstream of PAR-1b in both the establishment and maintenance of mammalian epithelial polarity. Current Biology: CB, 14(16), pp.1425-1435.

Tapon, N. & Hall, A, 1997. Rho, Rac and Cdc42 GTPases regulate the organization of the actin cytoskeleton. Current Opinion in Cell Biology, 9(1), pp.86-92.

Thyberg, J. & Moskalewski, S., 1985. Microtubules and the organization of the Golgi complex. Experimental Cell Research, 159(1), pp.1-16.

Tucker, R.W., Pardee, A.B. & Fujiwara, K., 1979. Centriole ciliation is related to quiescence and DNA synthesis in 3T3 cells. Cell, 17(3), pp.527-535.

Valetti, C. et al., 1999. Role of dynactin in endocytic traffic: Effects of dynamitin overexpression and colocalization with CLIP-170. Molecular Biology of the Cell, 10(12), pp.4107-4120.

Verhey, K.J. & Gaertig, J., 2007. The tubulin code. Cell Cycle, 6(17), pp.2152-2160.

Vinke, F.P., Grieve, A.G. & Rabouille, C., 2011. The multiple facets of the Golgi reassembly stacking proteins. The Biochemical Journal, 433(3), pp.423-433.

Vinogradova, T., Miller, P.M. & Kaverina, I., 2009. Microtubule network asymmetry in motile cells: role of Golgi-derived array. Cell Cycle (Georgetown, Tex.), 8(14), pp.2168-2174.

Wade, R.H. & Hyman, A.A., 1997. Microtubule structure and dynamics. Current Opinion in Cell Biology, 9(1), pp.12-17.

Wang, W. & Brautigan, D.L., 2008. Phosphatase inhibitor 2 promotes acetylation of tubulin in the primary cilium of human retinal epithelial cells. BMC Cell Biology, 9, p.62.

Watanabe, N. et al., 1997. p140mDia, a mammalian homolog of Drosophila diaphanous, is a target protein for Rho small GTPase and is a ligand for profilin. The EMBO Journal, 16(11), pp.3044-3056.

Watanabe, N. et al., 1999. Cooperation between mDia1 and ROCK in Rho-induced actin reorganization. Nature Cell Biology, 1(3), pp. 136-143.

Waterman-Storer, C. et al., 2000. Microtubules Remodel Actomyosin Networks in Xenopus Egg Extracts via Two Mechanisms of F-Actin Transport. The Journal of Cell Biology, 150(2), pp.361-376.

Waterman-Storer, C.M. & Salmon, E.D., 1997. Actomyosin-based Retrograde Flow of Microtubules in the Lamella of Migrating Epithelial Cells Influences Microtubule Dynamic Instability and Turnover and Is Associated with Microtubule Breakage and Treadmilling. The Journal of Cell Biology, 139(2), pp.417 -434.

Watts, J. L. et al., 2000. The C. elegans par-4 gene encodes a putative serine-threonine kinase required for establishing embryonic asymmetry. Development, 127(7), pp.1467 -1475.

Wehland, J. et al., 1983. The role of microtubules in the distribution of the Golgi apparatus: effect of taxol and microinjected anti-alpha-tubulin antibodies. Proceedings of the National Academy of Sciences, 80(14), pp. 4286-4290.

Wei, J.-H. & Seemann, J., 2010. Unraveling the Golgi ribbon. Traffic (Copenhagen, Denmark), 11(11), pp.1391-1400.

Wheatley, D.N., Wang, A.M. & Strugnell, G.E., 1996. Expression of primary cilia in mammalian cells. Cell Biology International, 20(1), pp.73-81.

Wittmann, T., Bokoch, G.M. & Waterman-Storer, C.M., 2003. Regulation of leading edge microtubule and actin dynamics downstream of Rac1. The Journal of Cell Biology, 161(5), pp.845 -851.

Xiang, Y. & Wang, Y., 2010. GRASP55 and GRASP65 play complementary and essential roles in Golgi cisternal stacking. The Journal of Cell Biology, 188(2), pp.237 -251.

Yadav, S. & Linstedt, A.D., 2011. Golgi positioning. Cold Spring Harbor Perspectives in Biology, 3(5). Available at: http://www.ncbi.nlm.nih.gov/pubmed/21504874.

Yoshimura, Y. & Miki, H., 2011. Dynamic regulation of GEF-H1 localization at microtubules by Par1b/MARK2. Biochemical and Biophysical Research Communications, 408(2), pp.322-328.

Young, K.G. et al., 2008. INF1 is a novel microtubule-associated formin. Molecular Biology of the Cell, 19(12), pp.5168-5180.

Zigmond, S., 2003. Formin-induced nucleation of actin filaments. Current Opinion in Cell Biology, 16, pp. 1-7.